GEOMETRIZED VACUUM PHYSICS. PART IX: "NEUTRINO"

FÍSICA DEL VACÍO GEOMETRIZADA. PARTE IX: "NEUTRINO"

Mikhail Batanov-Gaukhman[1]
(1) Moscow Aviation Institute (National Research University), Institute № 2 "Aircraft and rocket engines and power plants", st. Volokolamsk highway, 4, Moscow – Russia, 125993
(e-mail: alsignat@yandex.ru)

Recibido: 22/04/2024 - Evaluado: 31/05/2024 - Aceptado: 20/06/2024

ABSTRACT

In this article, based on exact solutions of the Einstein vacuum equation, are proposed metric-dynamic models of the electron and positron "neutrino" in the initial state, i.e. at the moment when it breaks away from the core of the corresponding "particle", and in the final state, when almost all the rotational energy of the initial "neutrino" is converted into its accelerated translational motion. It is shown that Riemannian geometry allows for the consideration of "neutrinos" of various scales: molecular "neutrinos", cluster "neutrinos", planetary "neutrinos", galactic "neutrinos", etc. The article proposes methods for generating "neutrinos" of various scales, convenient for conducting inexpensive experiments to clarify their properties. Of particular interest are "neutrinos" in the final state, since the metric-dynamic model of such a "neutrino" does not contain restrictions on the speed of its translational motion. That is, a "neutrino" in the final state does not have inertia, and theoretically can move at a speed significantly exceeding the speed of light. The article proposes a method for registering superluminal "neutrinos" in the final state.

RESUMEN

En este artículo, a partir de soluciones exactas de la ecuación de vacío de Einstein, se proponen modelos métrico-dinámicos del neutrino electrónico y positrónico en su estado inicial, es decir, en el momento en que se separa del núcleo de la partícula correspondiente, y en su estado final, cuando casi toda la energía rotacional del neutrino inicial se convierte en su movimiento de traslación acelerado. Se demuestra que la geometría de Riemann permite considerar neutrinos de diversas escalas: moleculares, de cúmulos, planetarios y galácticos, entre otros. El artículo propone métodos para generar neutrinos de diversas escalas, lo que facilita la realización de experimentos económicos para esclarecer sus propiedades. De particular interés son los neutrinos en estado final, ya que el modelo métrico-dinámico de estos neutrinos no impone restricciones a la velocidad de su movimiento de traslación. Es decir, un neutrino en estado final carece de inercia y, en teoría, puede moverse a una velocidad significativamente superior a la de la luz. El artículo propone un método para registrar neutrinos superlumínicos en estado final.

Keywords: neutrino, neutrino generation, geometrized physics, vacuum
Palabras clave: neutrino, generación de neutrinos, física geometrizada, vacío

BACKGROUND AND INTRODUCTION

This paper is the ninth in a series of articles under the general title "Geometrized Vacuum Physics (GVP) Based on the Algebra of Signature (AS)". The previous eight articles are listed in the bibliography (Batanov-Gaukhman, 2023a, 2023b, 2023c, 2023d, 2023e, 2023f, 2024a, 2024b; Shipov, 1998).

The paper (Batanov-Gaukhman, 2024b) presented metric-dynamic models of the outer shells of elementary "particles" moving uniformly and rectilinearly relative to the vacuum of which they themselves consist. In particular, the outer shell of a free valence "electron" moving translationally with a constant velocity V_z in the direction of the Z axis was represented by a complete set of Kerr metric-solutions with the signature $(+---)$ of the first Einstein vacuum equation $R_{ik} = 0$, see metrics (20) – (25) in (Batanov-Gaukhman, 2024b):

"ELECTRON"
moving rectilinearly and uniformly with velocity V_z in the direction of the Z axis

The outer shell of a free valence "electron", moving rectilinearly and uniformly (see Figure 1) (1)
the interval $[r_4, r_6]$, with the signature $(+---)$

I $$ds_1^{(+a1)2} = \left(1 - \frac{r_6 r}{\rho}\right) c^2 dt^2 - \frac{\rho dr^2}{\Delta^{(a)}} - \rho d\theta^2 - \left(r^2 + a_6^2 + \frac{r_6 r a_6^2}{\rho} sin^2\,\theta\right) sin^2\,\theta\, d\phi^2 + \frac{2r_6 r a_6}{\rho} sin^2\,\theta\, d\phi c dt, \quad (2)$$

H $$ds_2^{(+a2)2} = \left(1 - \frac{r_6 r}{\rho}\right) c^2 dt^2 - \frac{\rho dr^2}{\Delta^{(a)}} - \rho d\theta^2 - \left(r^2 + a_6^2 + \frac{r_6 r a_6^2}{\rho} sin^2\,\theta\right) sin^2\,\theta\, d\phi^2 - \frac{2r_6 r a_6}{\rho} sin^2\,\theta\, d\phi c dt, \quad (3)$$

V $$ds_3^{(+b1)2} = \left(1 + \frac{r_6 r}{\rho}\right) c^2 dt^2 - \frac{\rho dr^2}{\Delta^{(b)}} - \rho d\theta^2 - \left(r^2 + a_6^2 - \frac{r_6 r a_6^2}{\rho} sin^2\,\theta\right) sin^2\,\theta\, d\phi^2 + \frac{2r_6 r a_6}{\rho} sin^2\,\theta\, d\phi c dt, \quad (4)$$

H′ $$ds_4^{(+b2)2} = \left(1 + \frac{r_6 r}{\rho}\right) c^2 dt^2 - \frac{\rho dr^2}{\Delta^{(b)}} - \rho d\theta^2 - \left(r^2 + a_6^2 - \frac{r_6 r a_6^2}{\rho} sin^2\,\theta\right) sin^2\,\theta\, d\phi^2 - \frac{2r_6 r a_6}{\rho} sin^2\,\theta\, d\phi c dt; \quad (5)$$

The substrate of "electron"
uniformly and rectilinearly moving,
$r \in [0, \infty]$, signature $(+---)$

i $$ds_5^{(+)2} = c^2 dt^2 - \frac{\rho dr^2}{r^2 + a_6^2} - \rho d\theta^2 - (r^2 + a_6^2)\, sin^2\,\theta\, d\phi^2, \quad (6)$$

where $\rho = r^2 + a_6^2 cos^2\,\theta$, $\quad \Delta^{(a)} = r^2 - r_6\, r + a_6^2$, $\quad \Delta^{(b)} = r^2 + r_6\, r + a_6^2$,

$a_6 = \frac{r_6 V_z}{2c}$ – ellipticity parameter, where c is the speed of light. (7)

The analysis of the set of metrics (1) – (7), given in §4 in (Batanov-Gaukhman, 2024b), showed that in the outer shell of the moving "electron", i.e. in the vicinity of its core moving with a constant velocity, four intertwined laminar-toroidal-helical (laminar-turbulent) k-subcont (i.e. intra-vacuum, see (Batanov-Gaukhman, 2023a, 2023b, 2023c, 2023d, 2023e, 2023f, 2024a, 2024b)) vortices are induced, which on average are reduced to two counter-propagating laminar-toroidal-helical subcont vortices (see Figure 7a,b in (Batanov-Gaukhman, 2024b) or Figure 1a,b). These counter-propagating laminar-toroidal-helical subcont vortices on average completely compensate for each other's manifestation, and therefore are not observed (see Figure 1c). That is, in the outer shell of a moving "electron" there are both laminar subcont currents flowing out from its core and flowing to this core (see §2.2 in (Batanov-Gaukhman, 2024a)), as well as counter-rotational (turbulent) currents, which also, on average, compensate for the manifestations of the other. Thus, only the core of the "electron" moving with a constant speed V_z (see Figure 1c) can be observed (Batanov-Gaukhman, 2024b).

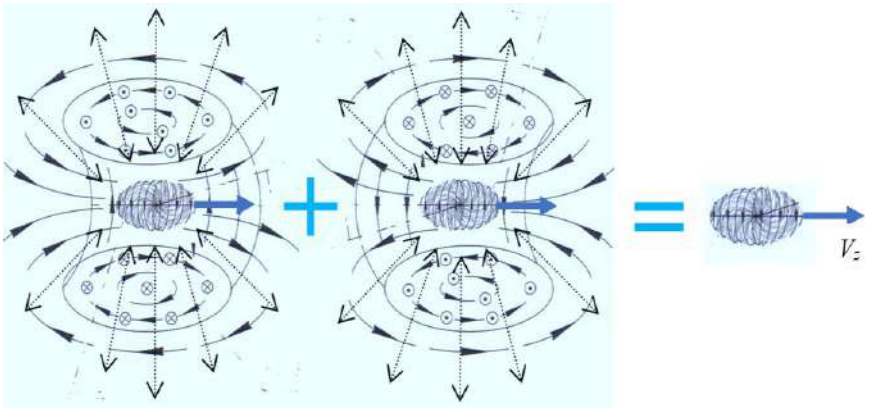

a) b) c)

Fig. 1: (Repetition of Figure 7 in (Batanov-Gaukhman, 2025b)). In the outer shell (more precisely in the vicinity of the core) of the "electron" moving with a constant velocity Vz on average, two counter toroidal-helical subcontact vortices and two counter (inflowing and outflowing) subcontact laminar currents are induced, which compensate each other's manifestations. Therefore, only the moving core of the "electron" can be observed

In this case, the metric-dynamic model of the outer shell of a free-valence "positron" moving rectilinearly and uniformly with a velocity V_z in the same direction of the Z axis is represented by a set of Kerr metric solutions of the first Einstein vacuum equation $R_{ik} = 0$ with the opposite signature (– + + +), see metrics (26) – (31) in (Batanov-Gaukhman, 2024b):

"POSITRON"
moving rectilinearly and uniformly with velocity V_z in the direction of the Z axis

The outer shell of a free valence "positron",
moving rectilinearly and uniformly (see Figure 2) (8)
in the interval [r_4, r_6], with the signature (– + + +)

H′ $$ds_1^{(-a1)2} = -\left(1-\frac{r_6 r}{\rho}\right)c^2dt^2 + \frac{\rho dr^2}{\Delta^{(a)}} + \rho d\theta^2 + \left(r^2 + a^2 + \frac{r_6 r a^2}{\rho}sin^2\,\theta\right)sin^2\,\theta\, d\phi^2 - \frac{2r_6 ra}{\rho}sin^2\,\theta\, d\phi cdt, \quad (9)$$

V $$ds_2^{(-a2)2} = -\left(1-\frac{r_6 r}{\rho}\right)c^2dt^2 + \frac{\rho dr^2}{\Delta^{(a)}} + \rho d\theta^2 + \left(r^2 + a^2 + \frac{r_6 r a^2}{\rho}sin^2\,\theta\right)sin^2\,\theta\, d\phi^2 + \frac{2r_6 ra}{\rho}sin^2\,\theta\, d\phi cdt, \quad (10)$$

H $$ds_3^{(-b1)2} = -\left(1+\frac{r_6 r}{\rho}\right)c^2dt^2 + \frac{\rho dr^2}{\Delta^{(b)}} + \rho d\theta^2 + \left(r^2 + a^2 - \frac{r_6 r a^2}{\rho}sin^2\,\theta\right)sin^2\,\theta\, d\phi^2 - \frac{2r_6 ra}{\rho}sin^2\,\theta\, d\phi cdt, \quad (11)$$

I $$ds_4^{(-b2)2} = -\left(1+\frac{r_6 r}{\rho}\right)c^2dt^2 + \frac{\rho dr^2}{\Delta^{(b)}} + \rho d\theta^2 + \left(r^2 + a^2 - \frac{r_6 r a^2}{\rho}sin^2\,\theta\right)sin^2\,\theta\, d\phi^2 + \frac{2r_6 ra}{\rho}sin^2\,\theta\, d\phi cdt; \quad (12)$$

The substrate of "electron"
uniformly and rectilinearly moving,
$r \in [0, \infty]$, signature (– + + +)

i $$ds_5^{(-)2} = -c^2dt^2 + \frac{\rho dr^2}{r^2+a^2} + \rho d\theta^2 + (r^2 + a^2)\,sin^2\,\theta\, d\phi^2. \quad (13)$$

The outer shell of a "positron" moving at a constant speed is completely analogous to the outer shell of a moving "electron" (see Figure 1), but in this case all *k*-antisubcont laminar and vortex processes proceed in the opposite direction (see Figure 2) and rotated (or phase-shifted) by 90^0 (see §5.2 in (Batanov-Gaukhman, 2023c)).

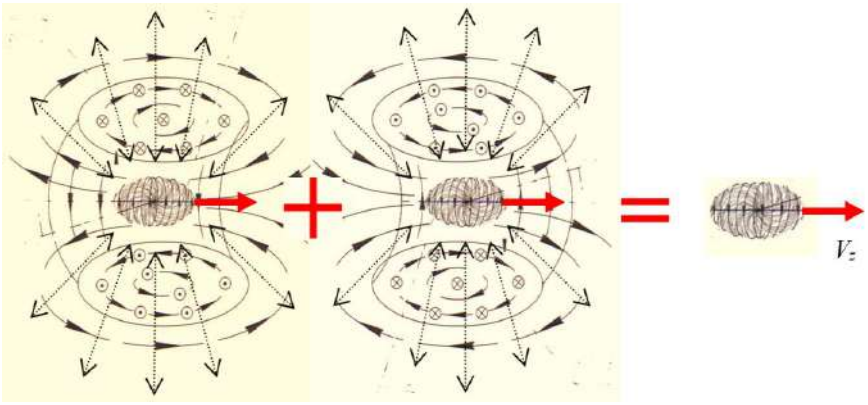

a) b) c)

Fig. 2: (Repetition of Figure 8 in (Batanov-Gaukhman, 2025b)). In the outer shell (more precisely in the vicinity of the core) of a "positron" moving with a constant velocity V_z on average, two counter toroidal-helical antisubcont vortices and two counter (inflowing and outflowing) antisubcont laminar currents are induced, which compensate for each other's manifestations. Therefore, only the moving core of the "positron" can be observed

In this article, we will consider the possibility of a metric-dynamic description of the electron "neutrino" and positron "neutrino". It is precisely these stable vacuum formations that were lacking in §4 in (Batanov-Gaukhman, 2023f) to complete the fully geometrized Standard Model of elementary "particles".

In addition, we will show that the existence of "neutrinos" of any scale is possible, for example: molecular "neutrinos", cellular "neutrinos", planetary "neutrinos", galactic "neutrinos", etc.

Beginning with the works of Wolfgang Pauli and Enrico Fermi, neutrinos have been the subject of extensive scientific literature (see, for example, (Ding *et al.*, 2022; Wolfenstein, 1978; Abi *et al.*, 2020; Babu *et al.*, 2020; Feruglio & Romanino, 2021; Kobayashi *et al.*, 2018; Criado & Feruglio, 2018; Mertens, 2016; Close, 2010; Balantekin, 2011; Winter, 2000; Cooper, 2022; Johnson & Tegen, 1999; Aničin, 2005; Kostelecký & Mewes, 2004; Gu *et al.*, 2016; King, 2017; Alfonso *et al.*, 2015; Kolbe *et al.*, 2004; Bellerive *et al.*, 2016; Abazajian *et al.*, 2012; Lasserre, 2014; Adamson, et al., MINOS Collaboration, 2007; Valentino *et al.*, 2023; Nomura & Popov, 2024; Andrew *et al.*, 2011; Worcester, 2023; Shao *et al.*, 2025; Lesgourgues & Pastor, 2006; Suematsu, 2024)), however, the author has not found a single geometrized model of neutrinos in serious journal publications. In this article, the model representations of neutrinos differ significantly from those generally accepted today, therefore the name of this particle is highlighted in quotation marks – "neutrino".

The peculiarities of the mathematical apparatus of the Algebra of signature inevitably force us to introduce new terminology, therefore, to understand what is written in this work, it is necessary to first familiarize yourself with the previous articles of this project (Batanov-Gaukhman, 2023a, 2023b, 2023c, 2023d, 2023e, 2023f, 2024a, 2024b).

MATERIALS AND METHOD

1 Analysis of the possible result of a collision of a moving elementary "particle" with a solid obstacle

In §5 in (Batanov-Gaukhman, 2023e) it was shown that four intertwined laminar-toroidal-helical (laminar-turbulent) subcont vortices, which are induced in the vicinity of the moving core of the "electron" (or "positron"), form a single geometrized electromagnetic field of toroidal type. If in that field we select only closed (ring-shaped) current lines (see Figures 3a and 8a), then only a double toroidal-helical vortex of the subcont will remain (i.e. the turbulent component of the subcont currents in the outer shell of the "electron", or a geometrized magnetic field of toroidal

type). This double toroidal-helical vortex of the subcont in the outer shell of the moving "electron" will be called the coupled electron e^-_{const}-"neutrino".

The bound electron e^-_{const}-"neutrino" always moves together with the core of the moving «electron» in the form of two double counter toroidal-helical vortices (see Figures 1 and 3a). The parameters of such a bound e^-_{const}-"neutrino" depend on the speed of the «electron» moving together with the core. But if the «electron» moves with a constant speed, then the parameters of the bound e^-_{const}-"neutrino" remain constant (const). Within the framework of the theory developed here, this bound electron e^-_{const}-"neutrino".is the light «particle» whose existence was predicted by Pauli to explain the apparent violation of the law of conservation of energy in beta decay.

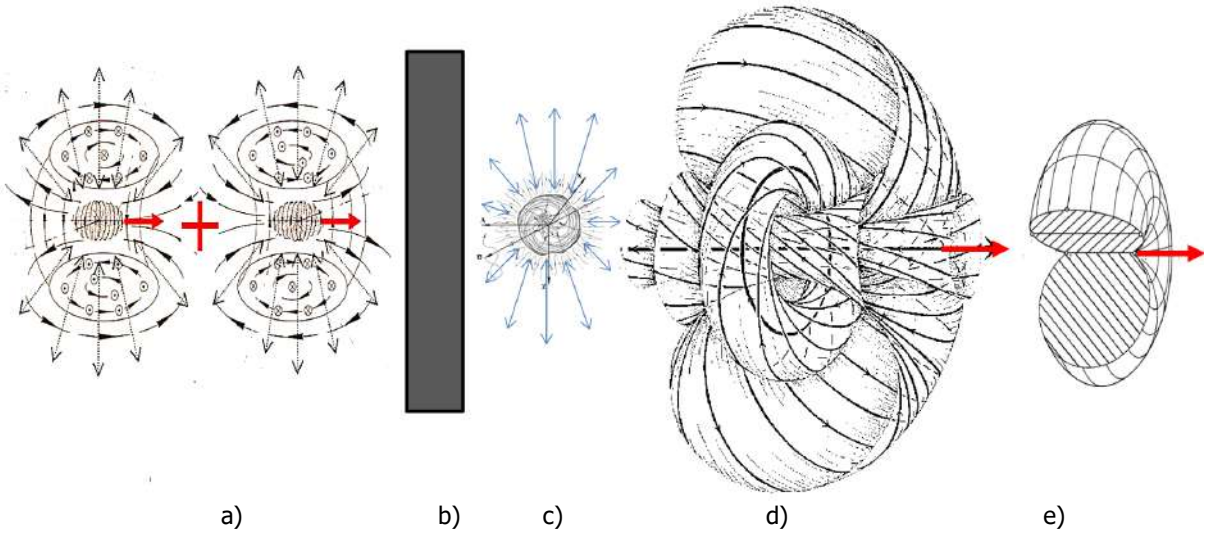

Fig. 3: An "electron" moving together with its associated (bound) e^-_{const}-"neutrino" (a), colliding with a solid obstacle (b), splits into a stationary "electron" (c) and a complex toroidal-helical vortex (d), continuing to move in the same direction with the same initial velocity V_z. This vortex, within the framework of the theory developed here, is the initial state of a free electron "neutrino"

Explanation of beta decay based on geometrized vacuum physics requires a separate study, taking into account the probabilistic description of random and quantum vacuum processes. This article only considers the possibility of the existence of free "neutrinos" and methods for their mathematical description.

Let a solid obstacle (see Figure 3*b*) appear on the path of the nucleus of an "electron" moving with the velocity V_z, the outer shell of which is described by the set of metrics (1) – (7) (see Figure 3a). Let a collision of the core of a moving "electron" with a solid obstacle result in it stopping abruptly and restoring its original spherical shape (see Figure 3c). In this case, the pairwise counter toroidal-helical motion of the subcont in the outer shell of the moving "electron" (i.e. the previously bound e^-_{const}-"neutrino") is torn off from its stopped core due to the inertia of rotation and continues moving in the same direction with the same initial velocity V_z in the form of a complex subcont formation resembling a spreading double toroidal-helical vortex (see Figure 3d).

Thus, as a result of the collision of a moving "electron" with a solid obstacle, a stationary "electron" and a complex double toroidal-helical vortex are formed, which we will call the initial state of the free electron "neutrino" (i.e. the initial free e^-_{const}-"neutrino").

To clarify the above, we present the metric (2) in expanded form

$$ds_1^{(+a1)2} = \left(1 - \frac{r_6 r}{r^2 + a_6^2 cos^2\theta}\right) c^2 dt^2 - \frac{r^2}{r^2 + a^2 - r r_6} dr^2 - \frac{a_6^2 cos^2\theta}{r^2 + a_6^2 - r r_6} dr^2 - r^2 d\theta^2 - a_6^2 cos^2\theta\, d\theta^2 - r^2 sin^2\theta\, d\phi^2 - \\ - \left(a_6^2 + \frac{r_6 r a_6^2 sin^2\theta}{r^2 + a_6^2 cos^2\theta}\right) sin^2\theta\, d\phi^2 + \frac{2 r_6 r a_6}{r^2 + a^2 cos^2\theta} sin^2\theta\, d\phi c dt. \quad (14)$$

Let's write this metric as two terms

$$ds_1^{(+a1)2} = ds_{1e}^{(+a1)2} + ds_{1n}^{(+a1)2},$$

where

$$ds_{1e}^{(+a1)2} = \left(1 - \frac{r_6 r}{r^2 + a_{6e}^2 cos^2\theta}\right) c^2 dt^2 - \frac{r^2}{r^2 + a_{6e}^2 - r r_6} dr^2 - r^2 d\theta^2 - r^2 sin^2\theta\, d\phi^2, \quad (15)$$

$$ds_{1n}^{(+a1)2} = 0 \cdot c^2 dt^2 - \frac{a_{6n}^2 cos^2\theta}{r^2 + a_{6n}^2 - r r_6} dr^2 - a_{6n}^2 cos^2\theta\, d\theta^2 - \left(a_{6n}^2 + \frac{r_6 r a_{6n}^2 sin^2\theta}{r^2 + a_{6n}^2 cos^2\theta}\right) sin^2\theta\, d\phi^2 + \frac{2 r_6 r a_{6n}}{r^2 + a_{6n}^2 cos^2\theta} sin^2\theta\, d\phi c dt. \quad (16)$$

$$a_{6e} = \frac{r_{6e} V_z}{2c} \quad (17)$$

is ellipticity parameter associated with the radius of the core of the moving "electron" r_{6e};

$$a_{6n} = \frac{r_{6n} V_{z1}}{2c} \quad (18)$$

is ellipticity parameter associated with the radius of the throat of the double toroidal-helical vortex r_{6n} induced around the core of the moving "electron".

If the subcont core and the double toroidal-helical vortex of the subcont induced around it move together, then $r_{6e} \approx r_{6n} \sim 10^{-13}$cm and, therefore, $a_{6e} \approx a_{6n} = a_6$.

When the previously moving core of the "electron" stops (see Figure 3c), i.e., when $V_z = 0$, the parameter a_{6e} (17) also tends to zero. Therefore, the first term (15) tends to the Schwarzschild metric

$$\lim_{a_{6e} \to 0} ds_{1e}^{(+a1)2} = \left(1 - \frac{r_6}{r}\right) c^2 dt^2 - \frac{dr^2}{\left(1 - \frac{r_6}{r}\right)} - r^2 (d\theta^2 + sin^2\theta\, d\phi^2). \quad (19)$$

The second term (16) defines the metric-dynamic model of an unstable toroidal-helical subcont formation, which continues to move by inertia in the same direction, but gradually dissolves in the vacuum as the parameter $a_{6n} = \frac{r_{6n} V_{z1}}{2c} \to 0$ decreases. In this case, the radius of the throat of this toroidal-helical vortex r_{6n} gradually increases, while its speed V_{z1} gradually decreases to zero ($V_{z1} \to 0$).

Therefore, the second term (16) describes a gradually dissolving subcont formation

(20)

$$ds_{1n}^{(+a1)2} = \lim_{a_{6n} \to 0} \left[0 \cdot c^2 dt^2 - \frac{a_{6n}^2 cos^2\theta}{r^2 + a_{6n}^2 - r r_{6n}} dr^2 - a_{6n}^2 cos^2\theta\, d\theta^2 - \left(a_{6n}^2 + \frac{r_{6n} r a_{6n}^2 sin^2\theta}{r^2 + a_{6n}^2 cos^2\theta}\right) sin^2\theta\, d\phi^2 + \frac{2 r_{6n} r a_{6n}}{r^2 + a_{6n}^2 cos^2\theta} sin^2\theta\, d\phi c dt\right] = 0.$$

It resembles a smoke ring in the air, which gradually slows down and expands as it moves away from its origin until it disappears completely (see Figure 4).

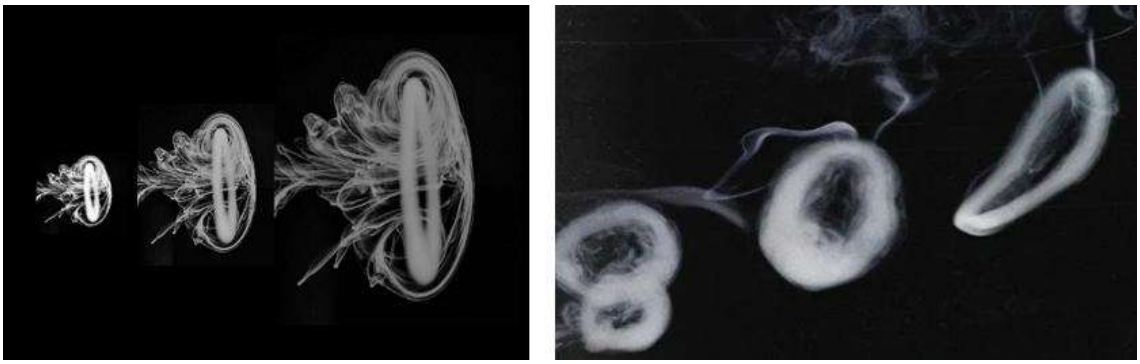

Fig. 4: Smoke rings gradually slow down and expand as they move away from the place where they originate

Doing similar actions with metric (5), we obtain

$$\lim_{a_{6e}\to 0} ds_{4e}^{(+b2)2} = \left(1+\frac{r_6}{r}\right)c^2dt^2 - \frac{dr^2}{\left(1+\frac{r_6}{r}\right)} - r^2(d\theta^2 + sin^2\,\theta\, d\phi^2), \tag{21}$$

$$ds_{4n}^{(+b2)2} = \lim_{a_{6n}\to 0}\left[0\cdot c^2dt^2 - \frac{a_{6n}^2cos^2\theta}{r^2+a_{6n}^2+rr_6}dr^2 - a_{6n}^2cos^2\theta\, d\theta^2 - \left(a_{6n}^2 - \frac{r_6ra_{6n}^2sin^2\,\theta}{r^2+a_{6n}^2cos^2\theta}\right)sin^2\,\theta\, d\phi^2 - \frac{2r_6ra_{6n}}{r^2+a_{6n}^2cos^2\theta}sin^2\,\theta\, d\phi cdt\right] = 0. \tag{22}$$

Thus, in the case of a collision of a moving "electron" with a solid obstacle (see Figure 3), from metrics (2) and (5) two metrics (19) and (21) remain

$$ds_{1e}^{(+a1)2} = \left(1-\frac{r_6}{r}\right)c^2dt^2 - \frac{dr^2}{\left(1-\frac{r_6}{r}\right)} - r^2(d\theta^2 + sin^2\,\theta\, d\phi^2), \tag{23}$$

$$ds_{4e}^{(+b2)2} = \left(1+\frac{r_6}{r}\right)c^2dt^2 - \frac{dr^2}{\left(1+\frac{r_6}{r}\right)} - r^2(d\theta^2 + sin^2\,\theta\, d\phi^2), \tag{24}$$

which describe the metric-dynamic state of the outer shell of a stopped (resting) valence "electron" (see metrics (24) – (25) in (Batanov-Gaukhman, 2024a)) (Figure 3c), and two metrics (20) and (22)

$$ds_{1n}^{(+a1)2} = \lim_{a_{6n}\to 0}\left[0\cdot c^2dt^2 - \frac{a_{6n}^2cos^2\theta}{r^2+a_{6n}^2-rr_{6n}}dr^2 - a_{6n}^2cos^2\theta\, d\theta^2 - \left(a_{6n}^2 + \frac{r_{6n}ra_{6n}^2sin^2\,\theta}{r^2+a_{6n}^2cos^2\theta}\right)sin^2\,\theta\, d\phi^2 + \frac{2r_{6n}ra_{6n}}{r^2+a_{6n}^2cos^2\theta}sin^2\,\theta\, d\phi cdt\right] = 0, \tag{20'}$$

$$ds_{4n}^{(+b2)2} = \lim_{a_{6n}\to 0}\left[0\cdot c^2dt^2 - \frac{a_{6n}^2cos^2\theta}{r^2+a_{6n}^2+rr_{6n}}dr^2 - a_{6n}^2cos^2\theta\, d\theta^2 - \left(a_{6n}^2 + \frac{r_{6n}ra_{6n}^2sin^2\,\theta}{r^2+a_{6n}^2cos^2\theta}\right)sin^2\,\theta\, d\phi^2 - \frac{2r_{6n}ra_{6n}}{r^2+a_{6n}^2cos^2\theta}sin^2\,\theta\, d\phi cdt\right] = 0, \tag{22'}$$

describing two counter toroidal-helical vortices of the subcont (see Figure 3d), which gradually slow down and spread out until they disappear completely.

In addition, there remain two metrics (2) and (3)

$$ds_{2n}^{(+a2)2} = \left(1-\frac{r_{6n}r}{r^2+a_{6n}^2cos^2\theta}\right)c^2dt^2 - \frac{(r^2+a_{6n}^2cos^2\theta)dr^2}{r^2+a_{6n}^2-r_{6n}r} - (r^2+a_{6n}^2cos^2\theta)d\theta^2 - \left(r^2+a_{6n}^2+\frac{r_{6n}ra_{6n}^2}{r^2+a_{6n}^2cos^2\theta}sin^2\,\theta\right)sin^2\,\theta\, d\phi^2 - \frac{2r_6ra_{6n}}{r^2+a_{6n}^2cos^2\theta}sin^2\,\theta\, d\phi cdt, \tag{2'}$$

$$ds_{3n}^{(+b1)2} = \left(1+\frac{r_{6n}r}{r^2+a_{6n}^2cos^2\theta}\right)c^2dt^2 - \frac{(r^2+a_{6n}^2cos^2\theta)dr^2}{r^2+a_{6n}^2+r_{6n}r} - (r^2+a_{6n}^2cos^2\theta)d\theta^2 - \left(r^2+a_{6n}^2-\frac{r_{6n}ra_{6n}^2}{r^2+a_{6n}^2cos^2\theta}sin^2\,\theta\right)sin^2\,\theta\, d\phi^2 + \frac{2r_6ra_{6n}}{r^2+a_{6n}^2cos^2\theta}sin^2\,\theta\, d\phi cdt, \tag{3'}$$

which describe the initial state of the other two counter toroidal-helical vortices of the subcont shown in Figure 3d, at the moment when they have just broken away from the stopped core of the "electron". They also continue to move in the original direction of the Z axis, but with increasing speed V_{z2}.

The zero components of the metric tensors from the metrics (2′) and (3′)

$g_{00}^{(+a1)} = \left(1 - \frac{r_{6n}r}{r^2+a_{6n}^2 cos^2\theta}\right)$ and $g_{00}^{(+b1)} = \left(1 + \frac{r_{6n}r}{r^2+a_{6n}^2 cos^2\theta}\right)$,

describe the laminar *a,b*-subcont currents that flow in and out of the core of the "electron" (see § 2.2 in (Batanov-Gaukhman, 2024a)). Therefore, in the double toroidal-helical vortex that has just moved away from the core of the stopped "electron", these currents are still present; as it moves away from the stopped core, they disappear (see Figure 3d). As a result, we come to the conclusion that this (second) double toroidal-helical vortex, which has just broken away and moved away a little, should be described not by the metrics (2′) and (3′), but by the metrics

$$ds_{2n}^{(+a2)2} = c^2dt^2 - \frac{(r^2+a_{6n}^2cos^2\theta)}{r^2+a_{6n}^2-r_{6n}r}dr^2 - (r^2+a_{6n}^2cos^2\theta)d\theta^2 - \left(r^2+a_{6n}^2+\frac{r_{6n}ra_{6n}^2}{r^2+a_{6n}^2cos^2\theta}sin^2\theta\right)sin^2\theta\, d\phi^2 - \frac{2r_6ra_{6n}}{r^2+a_{6n}^2cos^2\theta}sin^2\theta\, d\phi cdt, \quad (25)$$

$$ds_{3n}^{(+b1)2} = c^2dt^2 - \frac{(r^2+a_{6n}^2cos^2\theta)}{r^2+a_{6n}^2+r_{6n}r}dr^2 - (r^2+a_{6n}^2cos^2\theta)d\theta^2 - \left(r^2+a_{6n}^2-\frac{r_{6n}ra_{6n}^2}{r^2+a_{6n}^2cos^2\theta}sin^2\theta\right)sin^2\theta\, d\phi^2 + \frac{2r_6ra_{6n}}{r^2+a_{6n}^2cos^2\theta}sin^2\theta\, d\phi cdt. \quad (26)$$

2 Metric-dynamic model of the initial electron "neutrino"

2.1 Initial state of the electron "neutrino"

The above analysis allows us to collect metrics (16), (22), (25) and (26) into one system and construct the following metric-dynamic model of a double toroidal-helical vortex subcont formation that has just broken loose and moved a little away from the stopped valence "electron" (see Figure 3c,d). In the framework of the "Geometrized Physics of Vacuum" developed here, we will call such a vortex subcont formation the initial state of the electron "neutrino" (or the initial e_{start}^--"neutrino").

Electron "NEUTRINO"
in the initial state (e_{start}^--"neutrino")
in the interval $[r_{6n}, \infty]$, with the signature $(+ - - -)$

$$ds_{1n}^{(+a1)2} = 0\cdot c^2dt^2 - \frac{a_{6n1}^2cos^2\theta}{r^2+a_{6n1}^2-rr_{6n1}}dr^2 - a_{6n1}^2cos^2\theta\, d\theta^2 - \left(a_{6n1}^2+\frac{r_{6n1}ra_{6n1}^2sin^2\theta}{r^2+a_{6n1}^2cos^2\theta}\right)sin^2\theta\, d\phi^2 + \frac{2r_{6n1}ra_{6n1}}{r^2+a_{6n1}^2cos^2\theta}sin^2\theta\, d\phi cdt, \quad (27)$$

$$ds_{2n}^{(+a2)2} = c^2dt^2 - \frac{(r^2+a_{6n2}^2cos^2\theta)dr^2}{r^2+a_{6n2}^2-r_{6n2}r} - (r^2+a_{6n2}^2cos^2\theta)d\theta^2 - \left(r^2+a_{6n2}^2+\frac{r_{6n2}ra_{6n2}^2}{r^2+a_{6n2}^2cos^2\theta}sin^2\theta\right)sin^2\theta\, d\phi^2 - \frac{2r_{6n2}ra_{6n2}}{r^2+a_{6n2}^2cos^2\theta}sin^2\theta\, d\phi cdt, \quad (28)$$

$$ds_{3n}^{(+b1)2} = c^2dt^2 - \frac{(r^2+a_{6n2}^2cos^2\theta)dr^2}{r^2+a_{6n2}^2+r_{6n2}r} - (r^2+a_{6n2}^2cos^2\theta)d\theta^2 - \left(r^2+a_{6n2}^2-\frac{r_{6n2}ra_{6n2}^2}{r^2+a_{6n2}^2cos^2\theta}sin^2\theta\right)sin^2\theta\, d\phi^2 + \frac{2r_{6n2}ra_{6n2}}{r^2+a_{6n2}^2cos^2\theta}sin^2\theta\, d\phi cdt, \quad (29)$$

$$ds_{4n}^{(+b2)2} = 0\cdot c^2dt^2 - \frac{a_{6n1}^2cos^2\theta}{r^2+a_{6n1}^2+rr_{6n1}}dr^2 - a_{6n1}^2cos^2\theta\, d\theta^2 - \left(a_{6n1}^2-\frac{r_{6n1}ra_{6n1}^2sin^2\theta}{r^2+a_{6n1}^2cos^2\theta}\right)sin^2\theta\, d\phi^2 - \frac{2r_{6n1}ra_{6n1}}{r^2+a_{6n1}^2cos^2\theta}sin^2\theta\, d\phi cdt; \quad (30)$$

The substrate of electron "neutrino"
in the interval $[0, \infty]$

$$ds_5^{(+)2} = c^2dt^2 - dr^2 - r^2d\theta^2 - r^2\, sin^2\theta\, d\phi^2, \quad (31)$$

where

$$a_{6n1} = \frac{r_{6n1}V_{z1}}{2c} \quad (32)$$

is the ellipticity parameter of the first double toroidal-helical vortex of the subcont, with an increasing radius of the torus throat $r_{6n1}\rightarrow \infty$ and a decreasing velocity of translational motion $V_{z1}\rightarrow 0$ (see Figure 4);

$$a_{6n2} = \frac{r_{6n2}V_{z2}}{2c} \quad (33)$$

is the ellipticity parameter of the second double toroidal-helical vortex of the subcont, with a decreasing radius of the torus throat $r_{6n2}\rightarrow 0$ and an increasing velocity of translational motion $V_{z2}\rightarrow\infty$ (see Figure 3e).

Metrics (27) – (30) are not solutions of the Einstein vacuum equation $R_{ik} = 0$ (which are conservation laws, see Introduction in (Batanov-Gaukhman, 2023e)). According to (Batanov-Gaukhman, 2023e) this means that metrics (27) – (30) describe an unstable (temporary) subcont formation.

Analysis of the subcont velocity and acceleration field, performed similarly to §§ 4 and 5 in (Batanov-Gaukhman, 2024b), shows that metrics (27) – (30) describe two double toroidal-helical vortices. One of them (27) and (30) (or (20′) and (22′)) gradually stops and spreads out until it completely disappears. At the same time, the second double vortex (28) and (29) contracts and accelerates.

Both processes of electron "neutrino" propagation are interconnected, since jointly ensure the fulfillment of the vacuum balance requirement of the form: $(V_{z1} \to 0,\ r_{6n1} \to \infty)\ \&\ (r_{6n2} \to 0,\ V_{z2} \to \infty)$ (see Introduction to the article (Batanov-Gaukhman, 2023a)).

2.2 Accelerating part of the electron "neutrino"

Let's consider in more detail the second contracting double toroidal-helical vortex (28) and (29).

At the beginning of the independent motion of the second double toroidal-helical vortex (28) and (29), the radius of its throat r_{6n2} remains non-zero for some time due to the rotation inertia of the subcont. But gradually this throat inevitably contracts (i.e. $r_{6n2} \to 0$), filling the place of the missing core. Therefore, the terms containing r_{6n2} in the metrics (28) – (29) tend to zero. This, according to, for example, Exs. (45) in (Batanov-Gaukhman, 2024b)

$$v_r^{(+a1)} \equiv \lim_{r_{6n2}\to 0} c\sqrt{\frac{r_{6n2}r}{r^2+a_{6n2}^2 cos^2\theta}} = 0, \qquad v_\phi^{(+a1)} \equiv \lim_{r_{6n2}\to 0} \frac{cr_{6n2}a_{a_{6n2}}}{r^2+a_{6n2}^2 cos^2\theta} sin^2\theta = 0, \qquad v_\theta^{(+a1)} \equiv 0, \tag{34}$$

means that the mutually opposite (counter) rotation of the subcont in the considered region of the $\lambda_{-12,-15}$-vacuum gradually stops.

At the same time, the ellipticity parameter a_{6n2} can remain unchanged if the decrease in the radius of the throat of the second double toroidal-helical vortex r_{6n2} is accompanied by a proportional increase in the speed of its translational motion V_{z2} (i.e., with $r_{6n2} \to 0$, we obtain $V_{z2} \to \infty$), so that:

$$a_{6n2} = \lim_{\substack{r_{6n2}\to 0 \\ V_{z2}\to\infty}} \frac{r_{6n2}V_{z2}}{2c} = const. \tag{35}$$

Thus, after a sufficiently long period of time after the second double toroidal-helical vortex breaks away from the core of the stopped "electron", its throat contracts almost to zero (i.e. $r_{6n2} \to 0$), while the energetics of rotation of this vortex turns into an increase in the speed (i.e. of the energetics) of the translational motion of the second double toroidal-helical vortex ($V_{z2} \to \infty$). In this case, when $r_{6n2} \to 0$ and condition (35) is met, metrics (28) – (29) acquire the same simplified form

$$\lim_{\substack{r_{6n2}\to 0 \\ V_{z2}\to\infty}} ds_{2n}^{(+a2)2} = c^2dt^2 - \frac{(r^2+a_{6n2}^2 cos^2\theta)}{r^2+a_{6n2}^2} dr^2 - (r^2 + a_{6n2}^2 cos^2\theta)d\theta^2 - \left(r^2 + a_{6n2}^2\right) sin^2\theta\, d\phi^2, \tag{36}$$

$$\lim_{\substack{r_{6n2}\to 0 \\ V_{z2}\to\infty}} ds_{3n}^{(+b1)2} = c^2dt^2 - \frac{\left(r^2+a_{6n}^2 cos^2\theta\right)}{r^2+a_{6n}^2} dr^2 - \left(r^2 + a_{6n2}^2 cos^2\theta\right)d\theta^2 - \left(r^2 + a_{6n2}^2\right) sin^2\theta\, d\phi^2. \tag{37}$$

Metrics (36) and (37) are solutions of the Einstein vacuum equation $R_{ik} = 0$ (see (4) – (8) in (Batanov-Gaukhman, 2024b)). This means that they describe a stable subcont (i.e. intra-vacuum) formation, which we will call an electron "neutrino" in the final state (or a final e_{end}^--"neutrino").

Thus, we arrive at the following model of a final electron e^-_{end}-"neutrino" that is located at a large distance from the stopped valence "electron" (see Figure 3e).

Electron "NEUTRINO"
in the final state (e^-_{end}-"neutrino")
in the interval $[0, \infty]$, with the signature $(+ - - -)$

$$ds_n^{(+a)2} = c^2dt^2 - \frac{r^2+a_{6n2}^2cos^2\theta}{r^2+a_{6n}^2}dr^2 - (r^2 + a_{6n2}^2cos^2\theta)d\theta^2 - (r^2 + a_{6n2}^2)\,sin^2\,\theta\,d\phi^2 \quad -a\text{-субконт}, \quad (38)$$

$$ds_n^{(+b)2} = c^2dt^2 - \frac{r^2+a_{6n2}^2cos^2\theta}{r^2+a_{6n2}^2}dr^2 - (r^2 + a_{6n2}^2cos^2\theta)d\theta^2 - (r^2 + a_{6n2}^2)\,sin^2\,\theta\,d\phi^2 \quad -b\text{-субконт}; \quad (39)$$

The substrate of electron "neutrino"
in the interval [0, ∞]

$$ds_5^{(+)2} = c^2dt^2 - dr^2 - r^2d\theta^2 - r^2\,sin^2\,\theta\,d\phi^2, \quad (40)$$

where according to condition (34)

$$a_{6n2} = \lim_{\substack{r_{6n2}\to 0 \\ V_{z2}\to\infty}} r_{6n2}\frac{V_{z2}}{2c} = const \quad (41)$$

is ellipticity parameter of the final electron e^-_{end}-"neutrino" moving in the direction of the Z axis with the velocity $V_z \to \infty$ relative to the resting $\lambda_{\text{-}12,\text{-}15}$-vacuum, the disturbance of the outer side of which (i.e. subcont) it is.

The tendency of the translational motion velocity of e^-_{end}-"neutrino" to infinity ($V_{z2} \to \infty$) seems unacceptable, but in the mathematical model under consideration there is no limit on this velocity. Perhaps this model does not correspond to reality, but other metrics-solutions of the Einstein vacuum equation (i.e. stable vacuum formations) are not obtained in the case under consideration. The validity of this model can only be confirmed experimentally.

3 Metric-dynamic models of the positron "neutrino"

Performing actions similar to (14) – (41) with metrics (9) – (12), we obtain the following metric-dynamic models of the positron "neutrino".

Positron "NEUTRINO"
in the initial state (e^+_{start}-"neutrino")
in the interval $[r_{6n}, \infty]$, with the signature $(- + + +)$

$$ds_{1n}^{(-a1)2} = -0\cdot c^2dt^2 + \frac{a_{6n1}^2cos^2\theta}{r^2+a_{6n1}^2-rr_{6n1}}dr^2 + a_{6n1}^2cos^2\theta\,d\theta^2 + \left(a_{6n1}^2 + \frac{r_{6n1}ra_{6n1}^2sin^2\theta}{r^2+a_{6n1}^2cos^2\theta}\right)sin^2\,\theta\,d\phi^2 - \frac{2r_{6n1}ra_{6n1}}{r^2+a_{6n1}^2cos^2\theta}sin^2\,\theta\,d\phi cdt, \quad (42)$$

$$ds_{2n}^{(-a2)2} = -c^2dt^2 + \frac{(r^2+a_{6n2}^2cos^2\theta)dr^2}{r^2+a_{6n2}^2-r_{6n2}r} + (r^2 + a_{6n2}^2cos^2\theta)d\theta^2 + \left(r^2 + a_{6n2}^2 + \frac{r_{6n2}ra_{6n2}^2}{r^2+a_{6n2}^2cos^2\theta}sin^2\,\theta\right)sin^2\,\theta\,d\phi^2 + \frac{2r_{6n2}ra_{6n2}}{r^2+a_{6n2}^2cos^2\theta}sin^2\,\theta\,d\phi cdt, \quad (43)$$

$$ds_{3n}^{(-b1)2} = -c^2dt^2 - \frac{(r^2+a_{6n2}^2cos^2\theta)dr^2}{r^2+a_{6n2}^2+r_{6n2}r} + (r^2 + a_{6n2}^2cos^2\theta)d\theta^2 + \left(r^2 + a_{6n2}^2 - \frac{r_{6n2}ra_{6n2}^2}{r^2+a_{6n2}^2cos^2\theta}sin^2\,\theta\right)sin^2\,\theta\,d\phi^2 - \frac{2r_{6n2}ra_{6n2}}{r^2+a_{6n2}^2cos^2\theta}sin^2\,\theta\,d\phi cdt, \quad (44)$$

$$ds_{4n}^{(-b2)2} = -0\cdot c^2dt^2 + \frac{a_{6n1}^2cos^2\theta}{r^2+a_{6n1}^2+rr_{6n1}}dr^2 + a_{6n1}^2cos^2\theta\,d\theta^2 + \left(a_{6n1}^2 - \frac{r_{6n1}ra_{6n1}^2sin^2\theta}{r^2+a_{6n1}^2cos^2\theta}\right)sin^2\,\theta\,d\phi^2 + \frac{2r_{6n1}ra_{6n1}}{r^2+a_{6n1}^2cos^2\theta}sin^2\,\theta\,d\phi cdt; \quad (45)$$

The substrate of positron "neutrino"
in the interval [0, ∞]

$$ds_5^{(-)2} = -c^2dt^2 + dr^2 + r^2d\theta^2 + r^2\,sin^2\,\theta\,d\phi^2. \quad (46)$$

where

$$a_{6n1} = \frac{r_{6n1}V_{z1}}{2c} \quad (32')$$

is the ellipticity parameter of the first double toroidal-helical vortex of the antisubcont, with an increasing radius of the torus throat $r_{6n1} \to \infty$ and a decreasing velocity of translational motion $V_{z1} \to 0$ (see Figure 4);

$$a_{6n2} = \frac{r_{6n2}V_{z2}}{2c} \quad (33')$$

is the ellipticity parameter of the second double toroidal-helical vortex of the antisubcont, with a decreasing radius of the torus throat $r_{6n2} \to 0$ and an increasing velocity of translational motion $V_{z2} \to \infty$ (see Figure 3e).

Positron "NEUTRINO"

in the final state (e^{+}_{end}-"neutrino")

in the interval [0, ∞], with the signature (– + + +)

$$ds_n^{(-a)2} \approx -c^2dt^2 + \frac{r^2+a_{6n2}^2cos^2\theta}{r^2+a_{6n2}^2}dr^2 + (r^2 + a_{6n2}^2cos^2\theta)d\theta^2 + (r^2 + a_{6n2}^2)\,sin^2\,\theta\,d\phi^2 \quad -a\text{-субконт, (49)}$$

$$ds_n^{(-b)2} \approx -c^2dt^2 + \frac{r^2+a_{6n2}^2cos^2\theta}{r^2+a_{6n2}^2}dr^2 + (r^2 + a_{6n2}^2cos^2\theta)d\theta^2 + (r^2 + a_{6n2}^2)\,sin^2\,\theta\,d\phi^2 \quad -b\text{-субконт; (50)}$$

The substrate of positron "neutrino"

in the interval [0, ∞]

$$ds_5^{(+)2} = -c^2dt^2 + dr^2 + r^2d\theta^2 + r^2\,sin^2\,\theta\,d\phi^2, \quad (51)$$

where $a_{6n2} \approx \lim\limits_{\substack{r_{6n2}\to 0 \\ V_{z2}\to\infty}} r_{6n2}\frac{V_{z2}}{2c} = const$ (52)

is the ellipticity parameter of the final positron e^{+}_{end}-"neutrino" moving in the direction of the Z axis with the velocity $V_{z2} \to \infty$ relative to the resting $\lambda_{\text{-}12,\text{-}15}$-vacuum, a perturbation of the inner side of which (i.e. the antisubcont) it is.

4 Subcont deformations at the location of the final electron e^{-}_{end-}"neutrino"

Let's consider the subcont distortions in the vicinity of the location of the final e^{-}_{end}-"neutrino" (38) – (41).

We will judge the subcont deformations by the relative elongation of local sections of the outer side of the $\lambda_{\text{-}12,\text{-}15}$-vacuum (i.e. the subcont) (see Ex. (47) in (Batanov-Gaukhman, 2023c) and §2.8 in (Batanov-Gaukhman, 2023e))

$$l_i^{(+)} = \sqrt{\frac{g_{ii}^{(+)}}{g_{ii}^{0(+)}}} - 1. \quad (53)$$

First, as in §2.8.1 in (Batanov-Gaukhman, 2023e), we average the metrics (38) and (39)

$$ds_n^{(+ab)2} \approx \frac{1}{2}\left(ds_n^{(+a)2} + ds_n^{(+a)2}\right) \approx c^2dt^2 - \frac{r^2+a_{6n2}^2cos^2\theta}{r^2+a_{6n2}^2}dr^2 - (r^2 + a_{6n2}^2cos^2\theta)d\theta^2 - (r^2 + a_{6n2}^2)\,sin^2\,\theta\,d\phi^2. \quad (54)$$

We write out the averaged components of the metric tensor from the metric (54)

$$g_{00}^{(+)} = \frac{1}{2}\left(g_{00}^{(+a)} + g_{00}^{(+b)}\right) = 1, \qquad g_{11}^{(+)} = \frac{1}{2}\left(g_{11}^{(+a)} + g_{11}^{(+b)}\right) \approx -\frac{r^2+a_{6n2}^2\,cos^2\,\theta}{r^2+a_{6n2}^2}, \quad (55)$$

$$g_{22}^{(+)} = \frac{1}{2}\left(g_{22}^{(+a)} + g_{22}^{(+b)}\right) \approx -(r^2 + a_{6n2}^2\,cos^2\,\theta), \qquad g_{33}^{(+)} = \frac{1}{2}\left(g_{33}^{(+a)} + g_{33}^{(+b)}\right) \approx -(r^2 + a_{6n2}^2)\,sin^2\,\theta,$$

the rest $g_{ii}^{(+)} = 0$.

The components of the metric tensor $g_{00}^{0(+)}$, describing the uncurved (initial) state of the studied subcont region, are taken from the substrate metric (40):

$$g_{00}^{0(+)} = 1, \quad g_{11}^{0(+)} = -1, \quad g_{22}^{0(+)} = -r^2, \quad g_{33}^{0(+)} = -r^2 \sin^2\theta. \tag{56}$$

We substitute components (55) and (56) into the expression for the relative elongation (53). As a result, we obtain the following components of the relative elongation vector of the subcont at the location of e_{end}^{-}-"neutrino"

$$l_t^{(+)} \approx \sqrt{\frac{1}{1}} - 1 = 0, \tag{57}$$

$$l_r^{(+)} \approx \sqrt{\frac{r^2 + a_{6n2}^2 \cos^2\theta}{r^2 + a_{6n2}^2}} - 1, \tag{58}$$

$$l_\theta^{(+)} \approx \sqrt{1 + \frac{a_{6n2}^2 \cos^2\theta}{r^2}} - 1, \tag{59}$$

$$l_\phi^{(-)} \approx \sqrt{1 + \frac{a_{6n2}^2}{r^2}} - 1. \tag{60}$$

The graphs of functions (58) – (60) are shown in Figures 5 – 7.

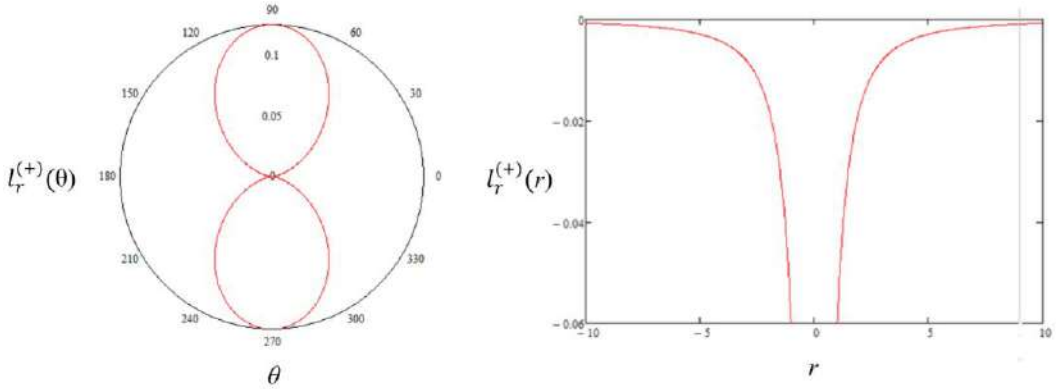

Fig. 5: The graphs of function (58) for $a_{6n2} = 0{,}5, \quad \theta = 50^0, \quad r = 0.09$

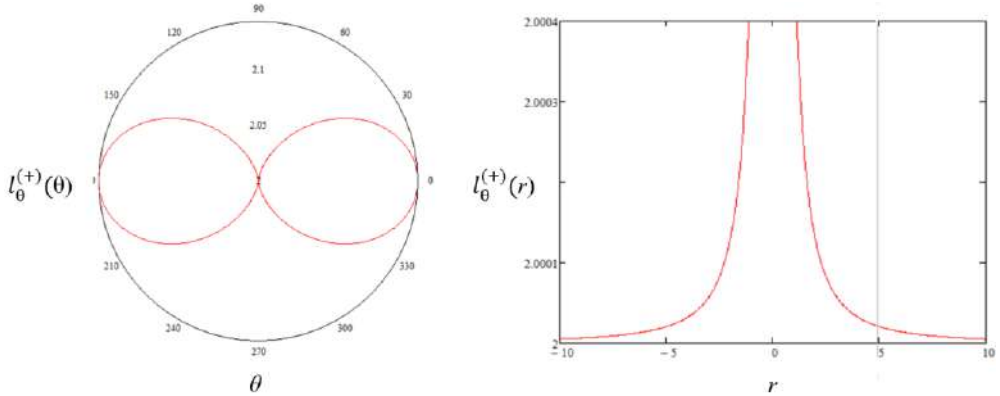

Fig.6: The graphs of function (59) for $a_{6n2} = 0{,}5, \quad \theta = 50^0, \quad r = 0.09$

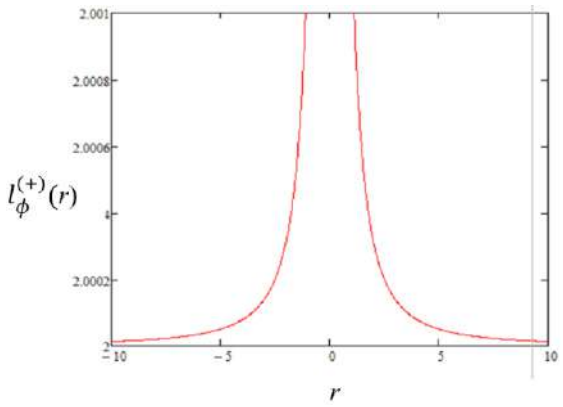

Fig.7: The graphs of function (60) for $a_{6n2}= 0{,}5$

An analysis of the graphs of functions (58) – (60), partly presented in Figures 5 – 7, leads to the conclusion that in the region of the location of the final e_{end}^{-}-"neutrino" moving with a constant velocity V_{z2}, the deformation of the subcont (i.e. the outer side of the $\lambda_{\text{-12,-15}}$-vacuum) corresponds to the shape of a toroid of rotation. Figures 3e and 8 show various attempts to illustrate the toroidal distortions of the subcont in the vicinity of the center of the final e_{end}^{-}-"neutrino".

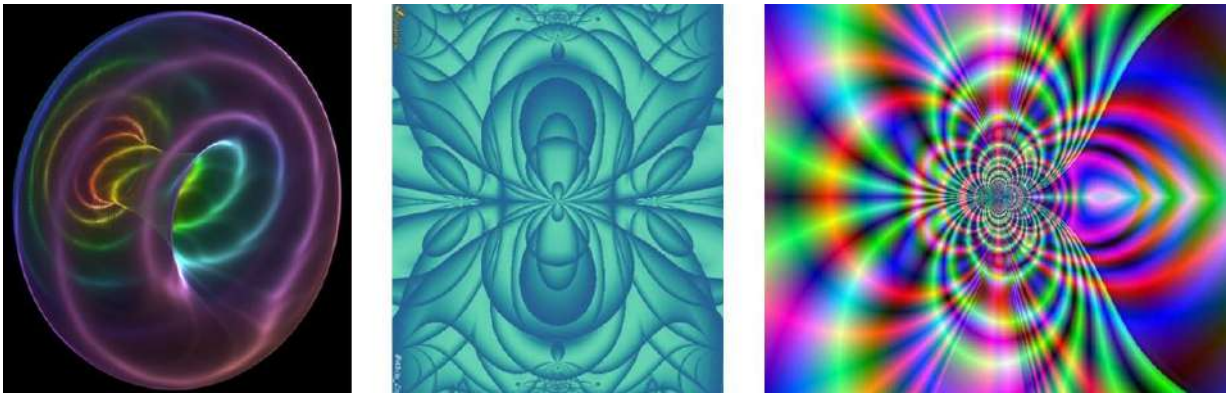

a) b) c)

Fig. 8: Attempts to illustrate the toroidal distortions of the outer side of the $\lambda_{\text{-12,-15}}$-vacuum (i.e., the subcont) in the vicinity of the center of the electron "neutrino" in the final state

At $a_{6n2} = 0$ (i.e., at V_{z2} = 0), all relative elongations (58) – (60) (i.e., deformations) of the subcont are equal to zero. Thus, the electron e_{end}^{-}-"neutrino" cannot exist without translational motion with some velocity V_{z2}.

Since the zero components of the metric tensors from the metrics (38) – (40) are approximately equal to

$$g_{00}^{(+\alpha)} \approx 1, \quad g_{01}^{(+\alpha)} = 0, \quad g_{02}^{(+\alpha)} = 0, \quad g_{03}^{(+\alpha)} \approx 0, \tag{61}$$

$$g_{00}^{(+b)} = 1, \quad g_{01}^{(+b)} = 0, \quad g_{02}^{(+b)} = 0, \quad g_{03}^{(+b)} = 0, \tag{62}$$

we have the relations

$$g_{r}^{(+a)} = -\frac{g_{01}^{(+a)}}{g_{00}^{(+a)}} \approx 0, \qquad g_{\theta}^{(+a)} = -\frac{g_{02}^{(+a)}}{g_{00}^{(+a)}} = 0, \qquad g_{\phi}^{(+a)} = -\frac{g_{03}^{(+a)}}{g_{00}^{(+a)}} \approx 0; \tag{63}$$

$$g_r^{(-b)} = -\frac{g_{01}^{(+b)}}{g_{00}^{(+b)}} = 0, \qquad g_\theta^{(-b)} = -\frac{g_{02}^{(+b)}}{g_{00}^{(+b)}} = 0, \qquad g_\phi^{(+b)} = -\frac{g_{03}^{(+b)}}{g_{00}^{(+b)}} = 0, \tag{64}$$

therefore, the final e_{end}^--"neutrino" practically lacks accelerated laminar and turbulent intra-vacuum currents (see §5.2 in (Batanov-Gaukhman, 2024b)):

$$B_{or}^{(+a)} = \frac{\gamma\sqrt{g_{00}^{(-a)}}}{2c\sqrt{|g|}}\left(\frac{\partial g_\phi^{(+a)}}{\partial\theta} - \frac{\partial g_\theta^{(-a)}}{\partial\phi}\right) \approx 0,$$
$$B_{o\theta}^{(+a)} = \frac{\gamma\sqrt{g_{00}^{(-a)}}}{2c\sqrt{|g|}}\left(\frac{\partial g_r^{(+a)}}{\partial\phi} - \frac{\partial g_\phi^{(+a)}}{\partial r}\right) \approx 0, \tag{65}$$
$$B_{o\phi}^{(-a)} = \frac{\gamma\sqrt{g_{00}^{(-a)}}}{2c\sqrt{|g|}}\left(\frac{\partial g_\theta^{(-a)}}{\partial r} - \frac{\partial g_r^{(-a)}}{\partial\theta}\right) = 0.$$

$$E_{or}^{(-a)} = -\gamma\frac{\partial\, ln\sqrt{g_{00}{}^{(-a)}}}{\partial r*} = 0,$$
$$E_{o\theta}^{(-a)} = -\gamma\frac{\partial\, ln\sqrt{g_{00}^{(-a)}}}{\partial\theta^*} = 0, \tag{66}$$
$$E_{o\phi}^{(-a)} = -\gamma\frac{\partial\, ln\sqrt{g_{00}^{(-a)}}}{\partial\phi^*} = 0.$$

$$E_{or}^{(-b)} = -\gamma\frac{\partial\, ln\sqrt{g_{00}{}^{(-b)}}}{\partial r*} = 0,$$
$$E_{o\theta}^{(-b)} = -\gamma\frac{\partial\, ln\sqrt{g_{00}^{(-b)}}}{\partial\theta^*} = 0, \tag{67}$$
$$E_{o\phi}^{(-b)} = -\gamma\frac{\partial\, ln\sqrt{g_{00}^{(-b)}}}{\partial\phi^*} = 0.$$

$$B_{or}^{(-b)} = \frac{\gamma\sqrt{g_{00}^{(-b)}}}{2c\sqrt{|g|}}\left(\frac{\partial g_\phi^{(-b)}}{\partial\theta} - \frac{\partial g_\theta^{(-ab)}}{\partial\phi}\right) = 0,$$
$$B_{o\theta}^{(-b)} = \frac{\gamma\sqrt{g_{00}^{(-b)}}}{2c\sqrt{|g|}}\left(\frac{\partial g_r^{(-b)}}{\partial\phi} - \frac{\partial g_\phi^{(-b)}}{\partial r}\right) = 0, \tag{68}$$
$$B_{o\phi}^{(-b)} = \frac{\gamma\sqrt{g_{00}^{(-a)}}}{2c\sqrt{|g|}}\left(\frac{\partial g_\theta^{(-b)}}{\partial r} - \frac{\partial g_r^{(-b)}}{\partial\theta}\right) = 0.$$

In the framework of the geometrized vacuum physics developed here, the electron "neutrino" in the final state (e_{end}^--"neutrino") (38) – (41) has virtually no inertial properties. In other words, we come to the need to consider the hypothesis that the electron e_{end}^--"neutrino" and positron e_{end}^+-"neutrino" in the final state are toroidal "phantoms" (or "shadows") that have virtually no inertia. Therefore, theoretically, they can move in a vacuum at a speed many times greater than the speed of light ($V_z >> c$). At the same time, it should be expected that they are virtually elusive, since they are very weak instantaneous "breezes" of vacuum disturbance (see Figure 8.1), which can be lost among vacuum fluctuations.

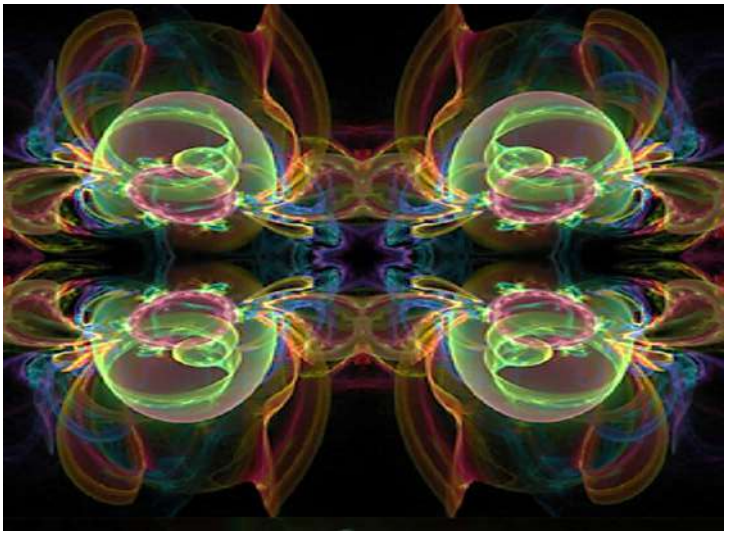

Fig. 8.1: Fractal illustration of electron and positron "neutrino" in the final state.
These are weak toroidal subcont-antisubcont "breaths",
i.e. (practically inertialess) vacuum disturbances

If it is possible to generate and detect these superluminal inertialess vacuum formations, then tasks can be set for organizing narrow-band communication channels with data transmission speeds significantly exceeding the speed of light.

5 Proton, planetary, galactic and other "neutrinos"

The metric-dynamic models of "neutrinos" (27) – (32) and (38) – (41) and "antineutrinos" (42) – (47) and (49) – (52) proposed in this article are suitable for describing similar vacuum formations and processes at various levels of the organization of the Universe. Similarly, meson, proton, neutron, nucleon, atomic, molecular and other "neutrinos" can be studied based on the metric-dynamic models of these stable and unstable vacuum formations proposed in the articles (Batanov-Gaukhman; 2023f; 2024a; 2024b).

For example, let us consider the final state of a proton "neutrino", which can break away from a sharply stopped core of the "proton" with topological configuration (92) in (Batanov-Gaukhman, 2023f):

$$\begin{array}{l} d_{\mathrm{r}}{}^{+}(+\ +\ +\ -) \\ u_{\mathrm{g}}{}^{-}(-\ +\ -\ +) \\ u_{\mathrm{b}}{}^{-}(-\ -\ +\ +) \\ p_{1}{}^{-}(-\ +\ +\ +)_{+} \end{array}$$

Within the framework of the theory developed here, the metric-dynamic model of such a proton "neutrino" in the final state has the form:

Proton "NEUTRINO" (69)

in the final state (p_{1end}^{-}-"neutrino") (see Figure 8.2)

in the interval [0, ∞], with the total signature (+ + + –) + (– + – +) + (– – + +) = (– + + +)

consists of:

$d_{\mathrm{r}}{}^{+}{}_{end}$-"neutrino"

with the signature (+ + + –)

$ds_{n1}^{(+a)2} \approx c^2dt^2 + \frac{r^2+a_{6n2}^2cos^2\theta}{r^2+a_{6n2}^2}dr^2 + (r^2 + a_{6n2}^2cos^2\theta)d\theta^2 - (r^2 + a_{6n2}^2)\,sin^2\,\theta\,d\phi^2$ – *a*-subcont,

$ds_{n2}^{(+b)2} \approx c^2dt^2 + \frac{r^2+a_{6n2}^2cos^2\theta}{r^2+a_{6n2}^2}dr^2 + (r^2 + a_{6n2}^2cos^2\theta)d\theta^2 - (r^2 + a_{6n2}^2)\,sin^2\,\theta\,d\phi^2$ – *b*-subcont;

$u_{\mathrm{g}}{}^{-}{}_{end}$-"neutrino"

with the signature (– + – +)

$ds_{n3}^{(-a)2} \approx -c^2dt^2 + \frac{r^2+a_{6n2}^2cos^2\theta}{r^2+a_{6n2}^2}dr^2 - (r^2 + a_{6n2}^2cos^2\theta)d\theta^2 + (r^2 + a_{6n2}^2)\,sin^2\,\theta\,d\phi^2$ – *a*-subcont,

$ds_{n4}^{(-b)2} \approx -c^2dt^2 + \frac{r^2+a_{6n2}^2cos^2\theta}{r^2+a_{6n2}^2}dr^2 - (r^2 + a_{6n2}^2cos^2\theta)d\theta^2 + (r^2 + a_{6n2}^2)\,sin^2\,\theta\,d\phi^2$ – *b*-subcont;

$u_{\mathrm{b}}{}^{-}{}_{end}$-"neutrino"

with the signature (– – + +)

$ds_{n5}^{(-a)2} \approx -c^2dt^2 - \frac{r^2+a_{6n2}^2cos^2\theta}{r^2+a_{6n2}^2}dr^2 + (r^2 + a_{6n2}^2cos^2\theta)d\theta^2 + (r^2 + a_{6n2}^2)\,sin^2\,\theta\,d\phi^2$ – *a*-subcont,

$ds_{n6}^{(4-b)2} \approx -c^2dt^2 - \frac{r^2+a_{6n2}^2cos^2\theta}{r^2+a_{6n2}^2}dr^2 + (r^2 + a_{6n2}^2cos^2\theta)d\theta^2 + (r^2 + a_{6n2}^2)\,sin^2\,\theta\,d\phi^2$ – *b*-subcont;

The substrate of proton "neutrino"

in the interval [0, ∞]

$ds_{7}^{(-)2} = -c^2dt^2 + dr^2 + r^2d\theta^2 + r^2\,sin^2\,\theta\,d\phi^2.$

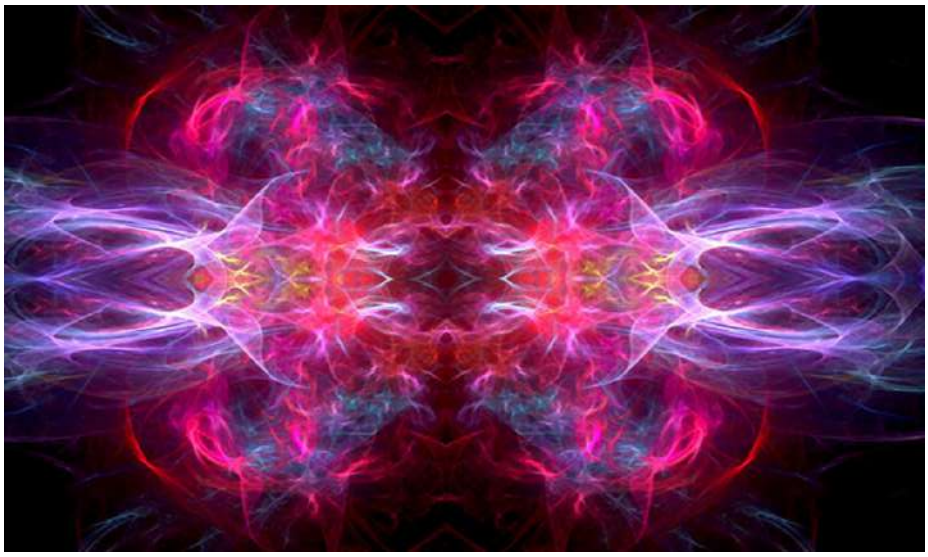

Fig. 8.2: Fractal illustration of proton and antiproton "neutrino" in the final state

If in all the equations of this article instead of $r_6 \sim 10^{-13}$ cm (the radius of the core of an elementary "particle", in particular the core of an "electron") we substitute any other radius from the hierarchy (44a) in (Batanov-Gaukhman, 2023f)

(70)

$r_1 \sim 10^{39}$ cm is radius commensurate with the radius of the mega-Universe;

$r_2 \sim 10^{29}$ cm is radius commensurate with the radius of the observable Universe;

$r_3 \sim 10^{19}$ cm is radius commensurate with the radius of the galactic core;

$r_4 \sim 10^{8}$ cm is radius commensurate with the radius of the core of a planet or star;

$r_5 \sim 10^{-3}$ cm is radius commensurate with the radius of a biological cell;

$r_6 \sim 10^{-13}$ cm is radius commensurate with the radius of an elementary particle core;

$r_7 \sim 10^{-24}$ cm is radius commensurate with the radius of a proto-quark core;

$r_8 \sim 10^{-34}$ cm is radius commensurate with the radius of a plankton core;

$r_9 \sim 10^{-45}$ cm is radius commensurate with the radius of the proto-plankton core;

$r_{10} \sim 10^{-55}$ cm is radius commensurate with the size of the instanton core,

then we get "neutrinos" of different scales.

Within the framework of the concepts developed here, a planetary "neutrino" or stellar "neutrino" is a toroidal magnetic field that has been torn off from a "planet" or a "star" (see Figure 9). Similarly, a galactic "neutrino" is a magnetized halo that has been torn off from a galaxy, etc.

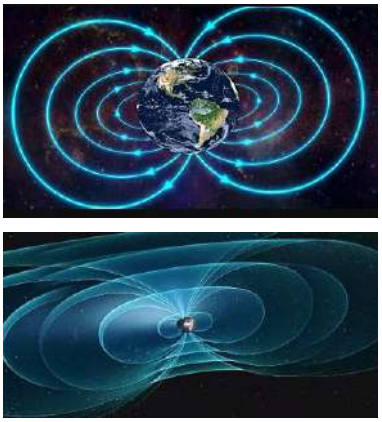

Fig. 9: Magnetic field of the planet

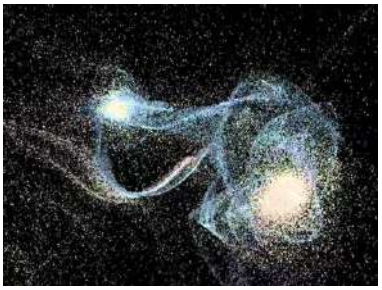

Fig. 10: Collision of galaxies

The cause of the formation of planetary "neutrinos" can be, for example, a collision of "planets", which can lead to the breakaway of their toroidal magnetic fields (see Figure 11).

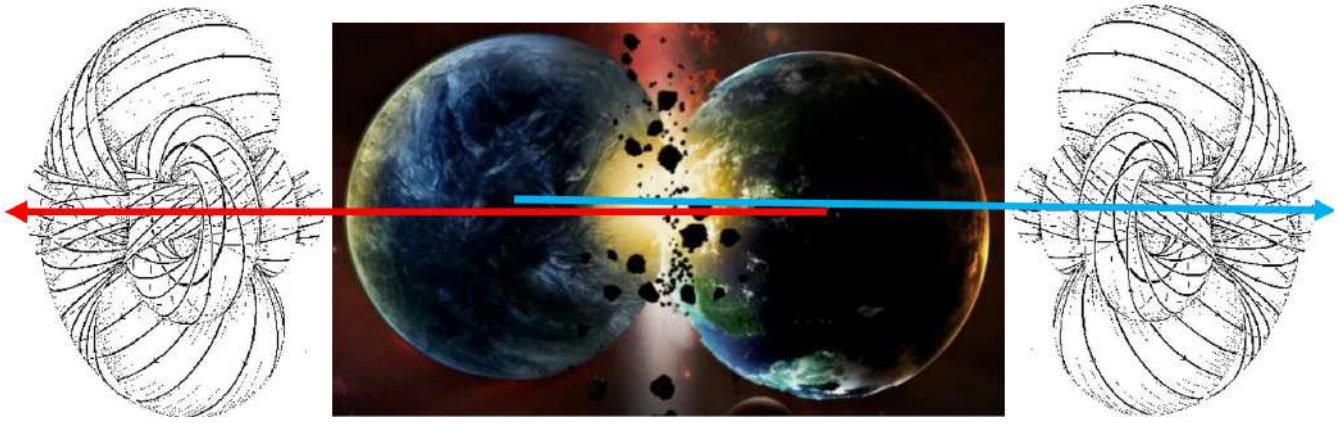

Fig. 11: Formation of planetary "neutrinos" (i.e. free toroidal magnetic fields) in the collision of two planets

Similarly, galactic "neutrinos" can be formed in the collision of two galaxies (see Figure 10).

6 Possibility of Generating "Neutrinos" of Different Scales

The above mathematical models of the electron "neutrino" and positron "neutrino" based on the metrics-solutions of the Einstein vacuum equation do not provide a complete picture of these quasi-stable vacuum formations. For example, the formulas do not limit the translational speed V_{z2} of the "neutrino" in the final state. It is unclear in what period of time the electron "neutrino" passes from the initial state (27) – (33) to the final state (38) – (41), etc.

To confirm the validity of the proposed mathematical model of the "neutrino" and to clarify its parameters, experimental behavior is necessary.

Below are possible methods of generating "neutrinos" suitable for experimental verification of the hypothesis presented here. In this case, we proceed from the fact that "neutrinos" of different scales (for example, electron, molecular, planetary and other "neutrinos") have a similar structure and properties.

6.1 Water "neutrinos". Volkov effect

Yuri Vasilyevich Volkov, an employee of the M. V. Lomonosov Moscow State University, often demonstrated the following experiment in the period 2001– 2009. He placed ampoules with twice-distilled water (bidistillate) for two weeks in a powerful magnetic field with an induction of about ~ 0.5 T. Then Yu.V. Volkov observed a number of the following effects with magnetized bidistillate (Batanov, 2006; Medvedeva & Panchelyuga, 2014; Bobrov, 2007):

- the weight of the ampoules with magnetized bidistillate increased $by \sim 2.2 \cdot 10^{-4}$ g;
- when a beam of red light (i.e. a beam from a regular laser pointer) was directed at the ampoules with magnetized bidistillate, the magnetized bidistillate lost its added weight within 1.5 – 2.5 minutes;
- an ampoule with magnetized bidistillate, placed on a foam raft on the surface of the water, moved in the direction of the source of the red beam of light (see Figure 12).
- when demagnetizing bidistillate with a red beam of light, radiation (of unclear nature) arose in the same direction as the laser pointer beam. This strange radiation had high penetrating power. Yu.V. Volkov placed various solid objects in the path of the red laser beam that passed through the ampoule with magnetized distillate. The barriers did not let the laser beam through. Nevertheless, the spectrometer installed behind the barriers recorded a flow of strange radiation, so intense that the sensitive element of this device failed.

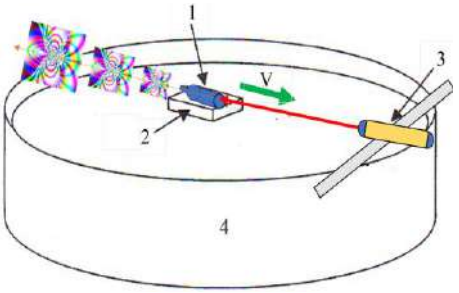

Fig. 12: Volkov's recoil effect consists of the movement of an ampoule with magnetized water in the direction of a source of red light (i.e., a laser pointer): 1 - ampoule with magnetized bidistillate water; 2 - foam plastic raft on the surface of the water; 3 - laser pointer illuminating the bottom of the ampoule; 4 - tank with water

Similar experiments were conducted under the supervision of A.V. Bobrov at the Oryol State Technical University Bobrov, 2007). In these experiments, barriers impenetrable to light were installed in the path of the laser beam. Nevertheless, various manifestations of some radiation were recorded behind the barrier, which A.V. Bobrov and his colleagues associated with the existence of a directed effect of a torsion field.

To explain the experiments of Volkov and Bobrov with magnetized water, the following hypothesis is proposed (Batanov, 2006). Many experiments conducted by various groups of researchers speak of the cluster structure of water (see, for example, (Marinov *et al.*, 2007)). Water clusters are generally understood to mean a bound state of about two billion water molecules. It is assumed that when distilled water is exposed to a powerful magnetic field for a long time, its clusters are deformed, and rotation of the intra-vacuum layers occurs around them, i.e., a magnetic field is induced (Figure 13).

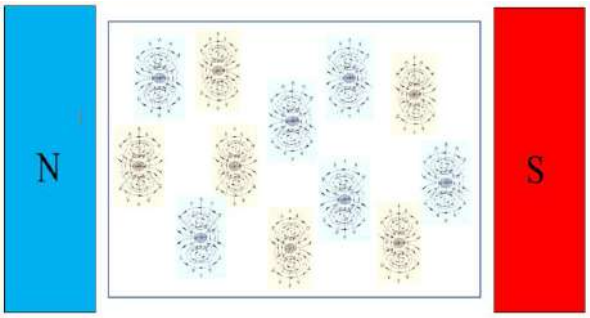

Fig. 13: Toroidal vacuum vortices (i.e. cluster magnetic fields) are induced in distilled water located between the poles of a magnet.

The wavelength of red light $\lambda \approx 6.5 \cdot 10^{-5}$ cm is comparable with the size of magnetized water clusters. Therefore, the beam of a laser pointer can stimulate the tearing off of vacuum toroidal vortices (i.e., essentially, toroidal magnetic fields, or water "neutrinos") from water clusters (see Figure 14). In this case, magnetic vortices (i.e., water "neutrinos") and water clusters repel each other (i.e., a recoil effect occurs).

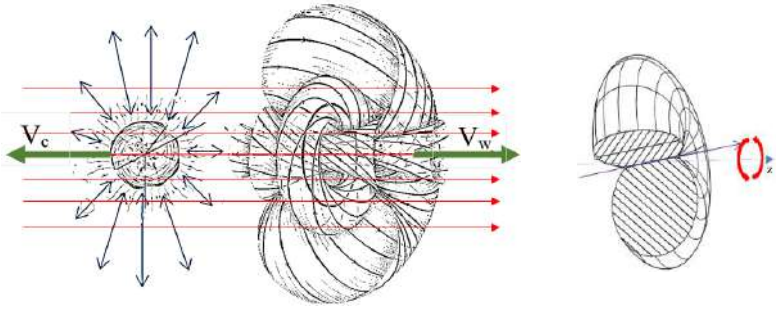

a) b)

Fig. 14: a) A red laser beam stimulates the tearing off of a vacuum toroidal vortex (i.e. a toroidal magnetic field, or water "neutrino") from a water cluster with a characteristic size of $\sim 5 \cdot 10^{-6}$ cm. In this case, the water cluster and the magnetic vortex repel each other, i.e. a recoil effect occurs. b) Illustration of the precession and nutation of the axis of rotation of the final water "neutrino" around the direction of its motion Z

The integral recoil effect, when a multitude of magnetic toroidal vortices (water "neutrinos") are torn off from various water clusters, can cause the movement of the ampoule with demagnetizing bidistilled water in the direction of the light beam source (see Figure 12).

If this hypothesis, explaining the Volkov recoil effect, turns out to be correct, then we will obtain a simple and experimentally accessible source of water "neutrinos". These "neutrinos" can be effectively used to study the properties of these quasi-stable vacuum formations.

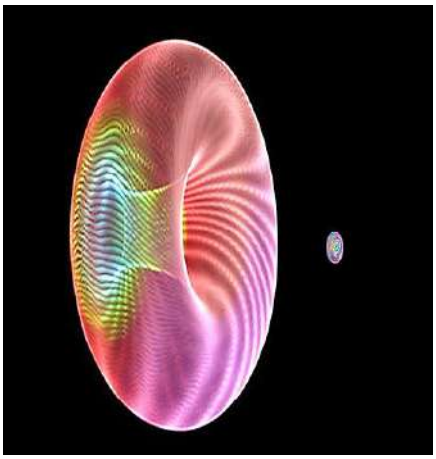

Fig. 15: Illustration of comparative sizes of water "neutrino" and electron "neutrino", the initial radii of the throats of which differ by 7 orders of magnitude

The throat of the water "neutrino" in the initial state is approximately seven orders of magnitude larger than the throat of the initial electron "neutrino", since the radii of the water cluster and the electron core differ by approximately 7 orders of magnitude ($r_w/r_e \approx 10^{-6}/10^{-13} \sim 10^7$). Otherwise, the water "neutrino" and the electron "neutrino" should not differ significantly from each other.

However, it should be expected that water "neutrinos" can interact with other "particles" with a significantly higher probability, since a noticeable interaction should occur only if the particles enter the throat of the initial "neutrino", where the vacuum currents are most concentrated, and their flow rates are maximum (see Figures 15 and 16).

On the other hand, the speeds of vacuum currents in the throat of the electron "neutrino" are significantly higher, and the concentration of current lines is significantly more intense than in the throat of the water "neutrino". Therefore, if, for example, the core of a free "electron" enters exactly the throat of the initial electron "neutrino", then such an interaction will be very strong, but unlikely, since the probability of such a hit is proportional to the cross-sectional area of the throat of the initial electron "neutrino" $\sim (10^{-13})^2 \approx 10^{-26}$ cm^2.

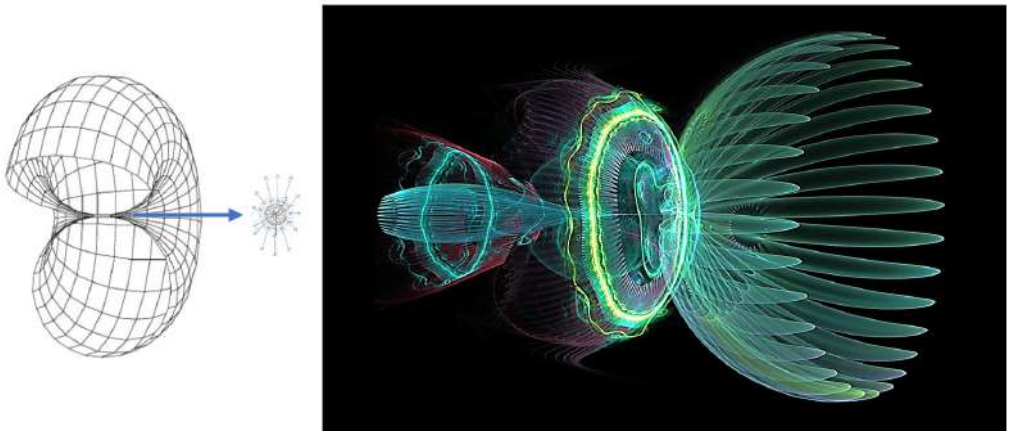

a) b)

Fig. 16: Illustration of the consequences of the collision of the core of an elementary "particle" with the throat of a "neutrino". *a*) Before the core of the "particle" hits the throat of a "neutrino"; *b*) After the core of the "particle" hits the throat of a "neutrino"

The probability of interaction of an electron "neutrino" with nuclei of other elementary particles can be estimated by the expression

$P_{en} \sim S_{en} \approx A_e \pi r_e^2$,

where A_e is the coefficient of interaction efficiency of an electron "neutrino" with core of other "particles".

Similarly, the probability of interaction of a water "neutrino" is estimated by the expression

$P_{wn} \sim S_{wn} \approx A_w \pi r_w^2$,

where A_w is the coefficient of interaction efficiency of a water "neutrino" with core of other "particles".

Under the condition $A_w \approx 100\ A_e$, a water "neutrino" can interact with core of other "particles" approximately 12 orders of magnitude more frequently than an electron "neutrino", because

$$P_{en} / P_{wn} \sim S_{wn} / S_{en} \approx A_w\, r_{wn}^2 / (A_e\, r_{en}^2) \sim 10^{12}. \quad (71)$$

An illustration of the possible consequences of the core of an elementary "particle" entering the throat of a "neutrino" is shown in Figure 16.

Water "neutrinos" (if their existence is confirmed experimentally) can be effectively used to develop new (possibly superluminal) technologies for transmitting information.

6.2 Coil "neutrino"

Another method for obtaining a macroscopic "neutrino" can be proposed. The magnetic field of a toroidal coil with direct current resembles a vacuum toroidal-helical vortex (see Figure 17).

If such a coil with current is forced to move progressively at high speed, and then suddenly braked (for example, by placing a solid obstacle in its path), then a coil "neutrino" can break away from such a coil.

The initial and final states of such a coil "neutrino" can be sets of metrics, for example, (27) – (33) and (38) – (41), respectively.

It should be expected that the initial radius of the throat of the coil "neutrino" is commensurate with the radius of the toroidal coil (see Figure 17).

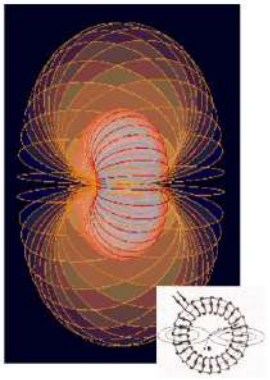

Fig. 17: Magnetic field of a toroidal coil with direct current

6.3 Current "neutrino"

It is possible that alternating electric current with high amplitude and high frequency can be the cause of the formation of electron and positron "neutrinos". In this case, if the change in the direction of movement of charges (in particular, "electrons" and "positrons") in a metal conductor occurs very quickly, then their abrupt stop before the change in the direction of movement can lead to the effect of tearing off toroidal magnetic fields (i.e. electron and positron "neutrinos", see Figure 20*a* in (Batanov-Gaukhman, 2024b)) from the cores of charged "particles".

7 Interaction of a finite electron e_{end}^--"neutrino" with an "electron" at rest

7.1 Metric-dynamic model of a free, quasi-rest, valence "electron"

Let's consider the following model of possible interaction of an "electron" at rest with a finite e_{end}^--"neutrino". If the finite electron e_{end}^--"neutrino" (described by the averaged metric (54)) hits exactly the center of the "electron" at rest, then instead of the extended model (2) – (10) in (Batanov-Gaukhman, 2024a), for a small time interval a

simplified metric-dynamic model of a quasi-at-rest "electron" can be constructed (see metrics (24) – (25) in (Batanov-Gaukhman, 2024a)):

"ELECTRON"

free, quasi-resting, valence

with signature (+ − − −), consisting of:

Outer shell

of a free, quasi-resting, valence "electron"

in the interval [r_2, r_6] (see Figure 1 in (Batanov-Gaukhman, 2025a))

$$ds_1^{(+)2} = \left(1 - \frac{r_6}{r}\right) c^2 dt^2 - \frac{dr^2}{\left(1 - \frac{r_6}{r}\right)} - r^2(d\theta^2 + sin^2\,\theta\, d\phi^2), \quad (72)$$

$$ds_2^{(+)2} = \left(1 + \frac{r_6}{r}\right) c^2 dt^2 - \frac{dr^2}{\left(1 + \frac{r_6}{r}\right)} - r^2(d\theta^2 + sin^2\,\theta\, d\phi^2); \quad (73)$$

Core

of a free, quasi-resting, valence "electron"

in the interval [0, r_6] (see Figure 1 in (Batanov-Gaukhman, 2025a))

$$ds_3^{(+)2} = -\left(1 + \frac{r^2}{r_6^2}\right) c^2 dt^2 - \frac{dr^2}{-\left(1 + \frac{r^2}{r_6^2}\right)} - r^2(d\theta^2 + sin^2\,\theta\, d\phi^2), \quad (74)$$

$$ds_4^{(+)2} = -\left(1 - \frac{r^2}{r_6^2}\right) c^2 dt^2 - \frac{dr^2}{-\left(1 - \frac{r^2}{r_6^2}\right)} - r^2(d\theta^2 + sin^2\,\theta\, d\phi^2); \quad (75)$$

The substrate

of free, quasi-resting, valence "electron",

i. e. $\boldsymbol{e_{end}^-}$**-"neutrino"**

in the interval [0, ∞]

$$ds_5^{(+)2} \approx c^2 dt^2 - \frac{r^2 + a_6^2 cos^2\theta}{r^2 + a_6^2} dr^2 - (r^2 + a_6^2 cos^2\theta) d\theta^2 - (r^2 + a_6^2)\, sin^2\,\theta\, d\phi^2, \quad (76)$$

where for brevity it is accepted

$a_6^2 = a_{6n2}^2 \approx r_{6n2}\frac{V_{z2}}{2c}$ is the ellipticity parameter of e_{end}^--"neutrino". (77)

By averaging metrics (72) and (73) (see §2.8 in (Batanov-Gaukhman, 2023e) and (27) in (Batanov-Gaukhman, 2025a)), we obtain for the case of a simplified metric-dynamic model of the outer shell of a quasi-static «electron»

$$ds_{1,2}^{(+)2} = \frac{1}{2}\left(ds_1^{(+)2} + ds_2^{(+)2}\right) = c^2 dt^2 - \frac{r^2}{r^2 - r_6^2} dr^2 - r^2 d\theta^2 - r^2\, sin^2\,\theta\, d\phi^2. \quad (78)$$

Similarly, averaging metrics (74) and (75), we have for the case of a simplified metric-dynamic model of the quasi-static "electron" core

$$ds_{3,4}^{(+)2} = \frac{1}{2}\left(ds_3^{(+)2} + ds_4^{(+)2}\right) = -c^2 dt^2 - \frac{dr^2}{\left(1 - \frac{r^4}{r_6^4}\right)} - r^2(d\theta^2 + sin^2\,\theta\, d\phi^2). \quad (79)$$

7.2 Deformations of the outer shell of a free, quasi-resting, valence "electron"

We will judge the deformations of the outer side of the λ-12,-15-vacuum (i.e. the subcont) in the outer shell (i.e. the outer side of the nucleus) of a free, quasi-resting, valence "electron" by the relative elongation (47) in (Batanov-Gaukhman, 2023c) (see also §2 in (Batanov-Gaukhman, 2024a))

$$l_i^{(+)} = \sqrt{1 + \frac{g_{ii}^{(+)} - g_{ii0}^{(+)}}{g_{ii0}^{(+)}}} - 1 = \sqrt{\frac{g_{ii}^{(+)}}{g_{ii0}^{(+)}}} - 1, \tag{79}$$

where in the case under consideration:
$g_{ii}^{(+)}$ is components of the averaged metric tensor curved section of the subcont in the outer shell of the quasi-static "electron";
$g_{ii0}^{(+)}$ is components of the metric tensor of the substrate (in this case e_{end}^{-}-"neutrino").

Substitute into Ex. (79) the components $g_{ii}^{(+)}$ from the averaged metric (78), and the components $g_{ii0}^{(+)}$ from the metric (76), as a result for the outer shell of the quasi-resting "electron" we obtain

$$l_t^{(+)} = 0, \qquad l_r^{(+)} = \sqrt{\frac{r^2(r^2 + a_{6)}^2}{(r^2 - r_6^2)(r^2 + a_6^2 cos^2\theta)}} - 1, \qquad l_\theta^{(+)} = \sqrt{\frac{r^2}{r^2 + a_6^2 cos^2\theta}} - 1, \qquad l_\phi^{(+)} = \sqrt{\frac{r^2 sin^2\theta}{(r^2 + a_6^2) sin^2\theta}} - 1. \tag{80}$$

The graphs of the relative elongation of the subcont in the vicinity of the core of a quasi-resting "electron" are shown in Figures 18 – 20.

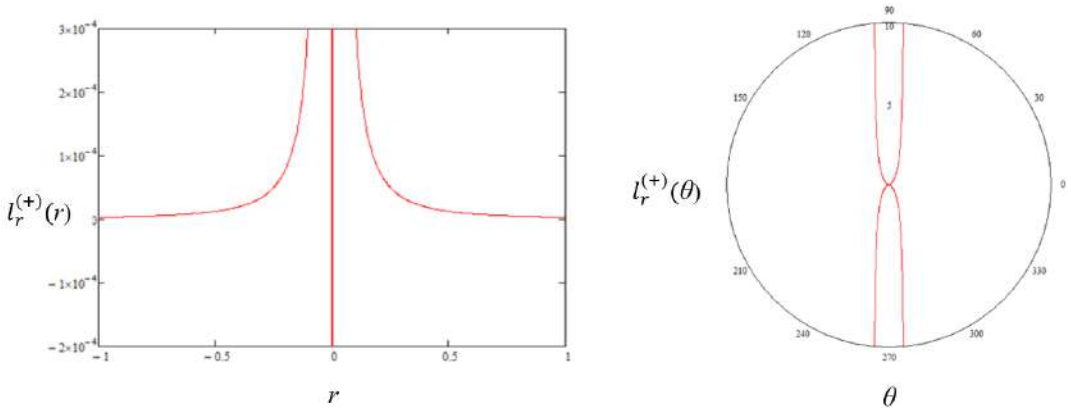

Fig. 18: Graphs of the function $l_r^{(+)}$ (80), for $a_6 = 0{,}005$, $r_6 = 5 \cdot 10^{-15}$, $\theta = 30^0$, $r = 5 \cdot 10^{-12}$

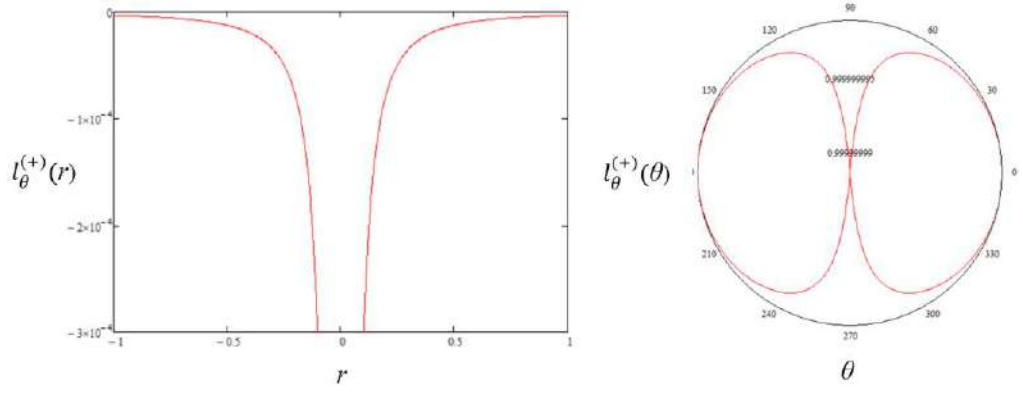

Fig. 19: Graphs of the function $l_\theta^{(+)}$ (80), for $a_6 = 0{,}005$, $r_6 = 5 \cdot 10^{-15}$, $\theta = 30^0$, $r = 5 \cdot 10^{-12}$

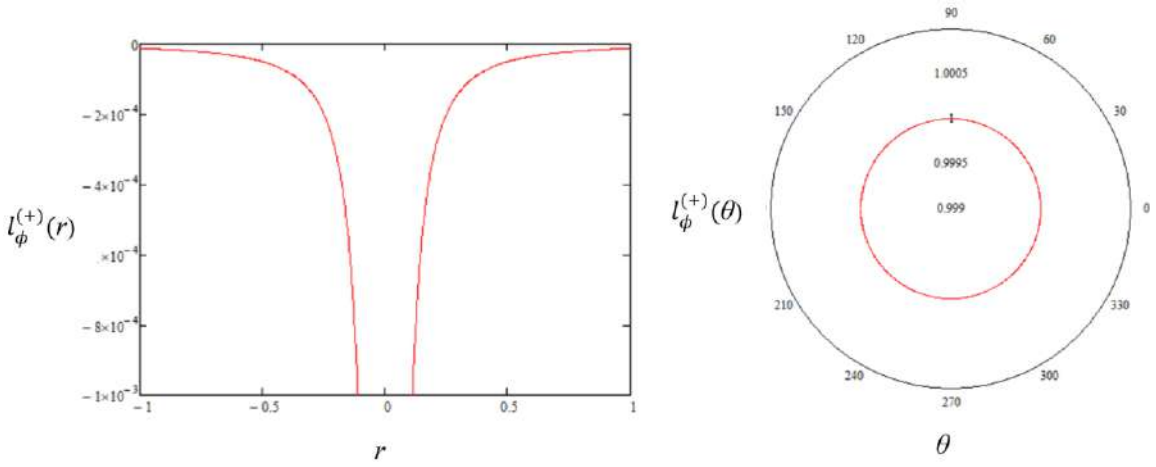

Fig. 20: Graphs of the function $l_{\phi}^{(+)}$ (80), for $a_6 = 0{,}005,\ r_6 = 5 \cdot 10^{-15},\ \theta = 30^0,\ \ r = 5 \cdot 10^{-12}$

7.3 Deformations of the core of a free, quasi-resting, valence "electron"

We substitute into expressions (79) the components $g_{ii}^{(+)}$ from the averaged metric (79), and the components $g_{ii0}^{(+)}$ from the metric (76), as a result for the core of a quasi-resting "electron", we obtain

$$l_t^{(+)} = 0, \qquad l_r^{(+)} = \sqrt{\frac{r_6^4(r^2 + a_{6)}^2}{(r_6^4 - r^4)(r^2 + a_6^2 cos^2\theta)}} - 1, \qquad l_{\theta}^{(+)} = \sqrt{\frac{r^2}{r^2 + a_6^2 cos^2\theta}} - 1, \qquad l_{\phi}^{(+)} = \sqrt{\frac{r^2 sin^2\theta}{(r^2 + a_6^2) sin^2\theta}} - 1. \qquad (81)$$

Graphs of the relative elongation of the subcont inside the core of the valence quasi-resting "electron" are shown in Figures 21 – 23.

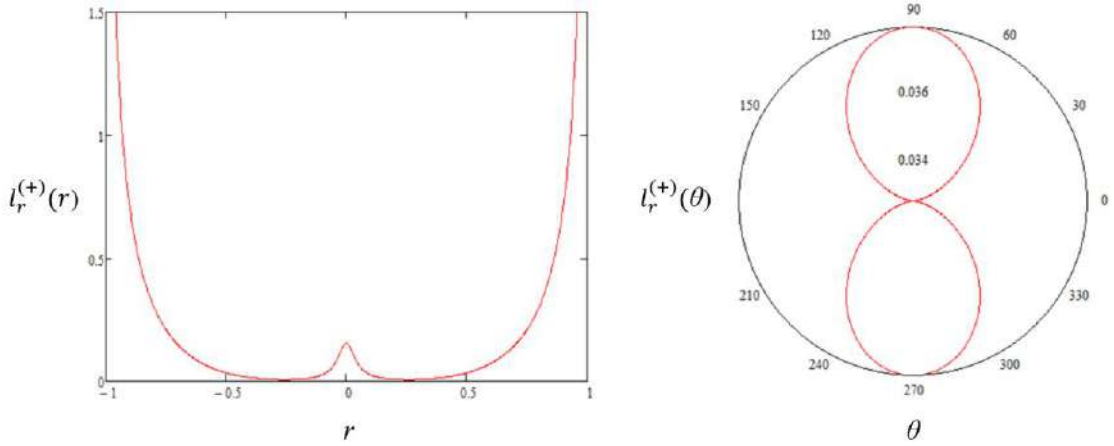

Fig. 21: Graphs of the function $l_r^{(+)}(81)$ for $a_6 = 0{,}05,\ r_6 = 1,\ \theta = 30^0,\ \ r = 0{,}5$

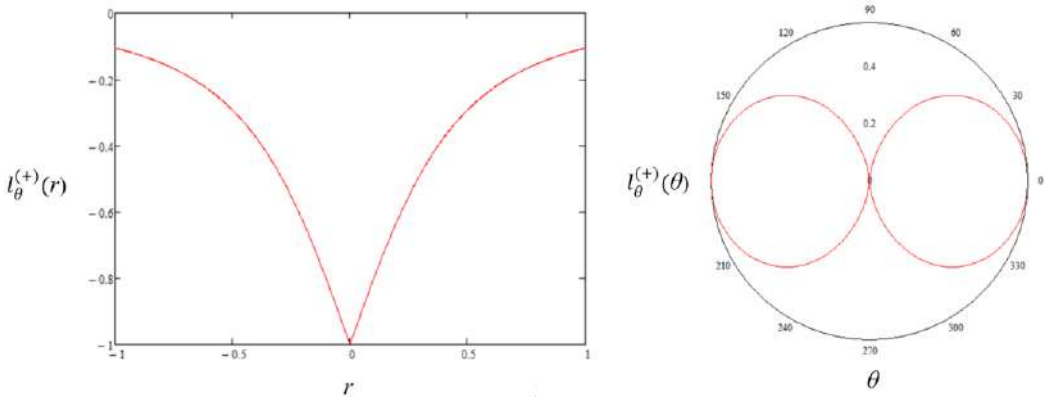

Fig. 22: Graphs of the function $l_\theta^{(+)}$ (81) for $a_6 = 1,\ r_6 = 1,\ \theta = 60^0,\ \ r = 0{,}5$

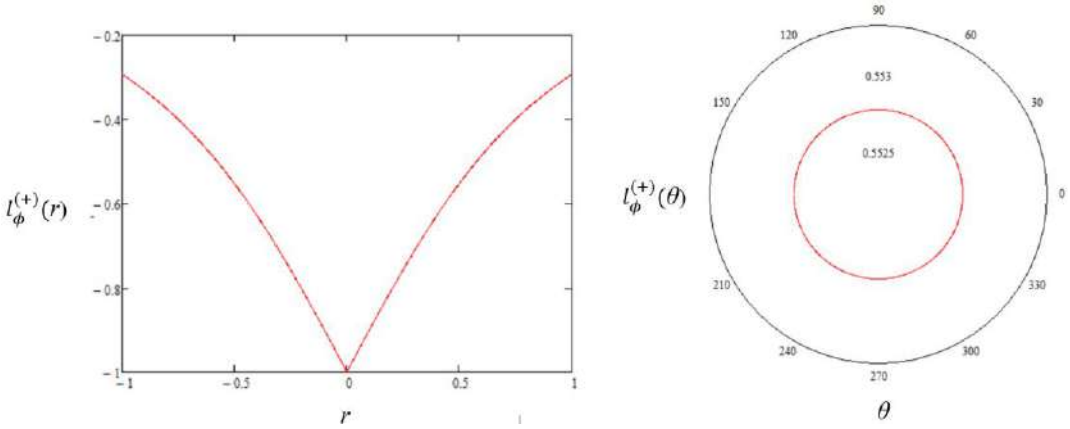

Fig. 23: Graphs of the function $l_\phi^{(+)}$ (81) for $a_6 = 1,\ r_6 = 1,\ \theta = 60^0,\ \ r = 0{,}5$

Comparing the graphs of relative elongations (80) and (81) presented in Figurs 18 – 23 with the corresponding graphs in Figurs 5 and 14 in (Batanov-Gaukhman, 2024a), we see that the quasi-resting valence "electron" (72) – (77) (i.e., the "electron" for which the shelt is the electron e_{end}^--"neutrino") differs significantly from the usual resting valence "electron" (1) – (10) in (Batanov-Gaukhman, 2024a) (at $r_2 \to \infty$ and $r_7 \to 0$). It is possible that these differences can be detected in experiments.

7.4 Quasi-resting, valence "planet"

It is very difficult to study a quasi-resting, valence "electron", since they are practically inaccessible to direct observation.

However, if in §7 we replace all $r_6 \sim 10^{-13}$ cm with $r_4 \sim 10^8$ cm (from the hierarchy (44a) in (Batanov-Gaukhman, 2023f) or (70)), then we obtain an approximate metric-dynamic description of a quasi-resting, valence "planet".

It is easier to observe a "planet" whose the substrate is a finite planetary PL_{end}^--"neutrino". But the question remains open: - "How likely is it that a quasi-resting "planet" will appear in our field of vision?"

CONCLUSION

In this ninth part of the "Geometrized Vacuum Physics (GVP) based on the Algebra of Signature (AS)" metric-dynamic models of "neutrino" are proposed. This is a geometrized model of the last "particle" that was missing in §4 in (Batanov-Gaukhman, 2023f) to complete the fully geometrized Standard Model of elementary "particles".

In the theory developed here, "neutrino" is, in essence, a double toroidal-helical geometrized magnetic field (more precisely, two counter toroidal-helical vortices of the subcont, see Figures 1 and 3a), induced around the core of a moving "particle" (in particular, an "electron" or "positron"), considered in the article (Batanov-Gaukhman, 2024b).

In some cases, for example, when an "electron" moving at high speed suddenly stops (Fig. 3c), then the double toroidal-helical vortex of the subcont (i.e. the outer side of the $\lambda_{\text{-12,-15}}$-vacuum) can break away from the core of the stopped "electron" and continue moving in the same direction (see Figure 3d). This independent vacuum formation is called in this article an electron "neutrino" in the initial state (or an initial electron "neutrino", abbreviated e^-_{start}-"neutrino").

The independent existence of e^-_{start}-"neutrino" is connected with the inertia of the rotational motion of the subcont in the counter toroidal-helical vortex. That is, the rotation of the subcont cannot stop immediately.

At the same time, e^-_{start}-"neutrino" is not a stable vacuum formation. Metrics (27) – (32), defining the metric-dynamic model of e^-_{start}-"neutrino", are not solutions of the vacuum Einstein equation, which expresses geometrized conservation laws.

Over time, the free e^-_{start}-"neutrino" is divided into two counter toroidal-helical vortices of the subcont.

One of them, moving away from the core of the stopped "electron" (i.e. from the starting point), increases in size and slows down until it completely dissolves in the fluctuating vacuum (like smoke rings in the air, see Figure 4).

The throat of the second double counter toroidal-helical vortex, on the contrary, gradually narrows down to almost zero over time, while its rotation gradually stops, and the speed of its translational motion increases more and more (see Figure 8). The inertia (or geometrized energy) of the rotational motion of the subcont in the second double counter vortex of the subcont gradually turns into an acceleration of the translational motion of this quasi-stable vacuum formation as a whole. As a result, over time, the rotation of the subcont in e^-_{start}-"neutrino" almost completely stops, while a stable deformation of the subcont of the toroidal type (e^-_{end}-"neutrino") remains (see Figure 8c), which moves at a speed significantly exceeding the speed of light. More precisely, the metric-dynamic model of the final state of a free electron e^-_{end}-"neutrino" (38) – (41) proposed in this article has no restrictions on the speed of its translational movement in a stationary $\lambda_{\text{-12,-15}}$-vacuum, the moving deformation of the outer side of which it itself is.

The final e^-_{end}-"neutrino" is like an instantly flying «breath» (practically an inertialess «phantom», see Figure 8c), which almost does not interact with other stable vacuum formations (elementary «particles»). However, if some «particle» (for example, an «electron») captures the final electron e^-_{end}-"neutrino" (i.e. if this toroidal «breath» for some reason becomes a substrate of such a «particle»), then such a connection can be interpreted as an interaction of the e^-_{end}-"neutrino"with the «particle», which, as shown in §7, should lead to quite noticeable consequences.

Many scientific articles are devoted to the mass of neutrinos, for example, (Ding *et al.*, 2022; Mertens, 2016; Gu *et al.*, 2016; Worcester, 2023; Shao *et al.*, 2025). In the framework of the Geometricized Vacuum Physics (GVP), proposed in a series of articles (Batanov-Gaukhman; 2023a, 2023b, 2023c, 2023d, 2023e, 2023f, 2024a, 2024b) and in this article, the concept of "mass" is absent, since it is in principle impossible to introduce the dimension of

kilogram into a completely geometrized theory. However, the analogue of the inertial mass in GVP is the integral inertia of the accelerated linear (laminar) and rotational (turbulent) motion of $\lambda_{m,\text{n}}$-vacuum layers (see §7.2 in (Batanov-Gaukhman, 2023c) and §§4,5,6 in (Batanov-Gaukhman, 2023d)).

In this article it was found that the inertial properties of the "neutrino" depend on its state. For example, the electron "neutrino" in different situations has different integral (total) inertia.

In the case of a bound electron e^-_{const}-"neutrino", the speeds and accelerations of the subcont participating in this binary-counter (i.e. 4-layer) toroidal-helical vortex around the moving core of the "electron" (see Figures 1 and 3*a*) depend on the constant speed V_z, of this entire stable vacuum formation. This means that the integral inertia (analog of mass) of this e^-_{const}-"neutrino" is constant, but depends on the velocity V_z.

The initial free electron e^-_{start}-"neutrino", i.e. the double toroidal-helical vortex subcont formation, which has just broken away and moved a little away from the stopped valence "electron" (see Figure 3*d*), although in total it has a constant initial integral inertia, but this inertia is internally rebuilt. That is, part of this integral inertia is dissipated in the vacuum together with the expanding double toroidal-helical vortex (like a smoke ring in the air, Figures 3*d* and 4), and the second part of the initial inertia e^-_{start}-"neutrino" passes from the counter-rotating accelerated motion of the subcont in the second toroidal-helical vortex, with a constantly decreasing radius of its throat, into the accelerated translational motion of this entire toroidal subcont formation as a whole (see Figure 3*d*).

The final free electron e^-_{end}-"neutrino" (see Figures 3e and 8c) has virtually no rotational inertia. In this state, virtually all of the initial toroidal-helical rotation of the subcont has transformed into translational motion of the free e^-_{end}-"neutrino" with a velocity many times greater than the speed of light ($V_z >> c$). That is, the final free electron e^-_{end}-"neutrino" is a virtually non-rotating toroidal deformation of the outer side of the $\lambda_{\text{-12,-15}}$-vacuum (i.e. the subcont, Figure 8c), while it has virtually no potential inertia of the subcont tension, since it is described by metrics (38) and (39), which are solutions of the Einstein vacuum equation for space with flattened coordinates. That is, the final free e^-_{end}-"neutrino" is practically a «phantom» (ghost, shadow), but not quite a shadow, and this gives hope of detecting it.

The study of methods for the emission and detection of free finite (i.e. practically inertialess) "neutrinos" is an important task, since the development of this vacuum technology can lead to the possibility of transmitting data via a wireless narrow-beam communication channel, over huge distances, with high penetrating power, noise immunity and at speeds significantly exceeding the speed of light. This does not violate the principles of the theory of relativity, since a free "neutrino" in the final state is practically like a shadow, and an inertialess shadow can move with any speed.

In §§5 and 6, several methods for the artificial generation of "neutrinos" of various scales are proposed, which can be used for the experimental study of their properties.

The metric-dynamic models of "neutrinos" proposed in this article are based on exact solutions of the Einstein vacuum equation, i.e., intended to describe stable vacuum formations. Free "neutrinos" of any scale and any type are not stable objects; they are constantly changing, striving for an infinitely long time to reach a final stable state. We assumed that "neutrinos" change slowly enough to consider them as quasi-stable toroidal formations, i.e., we applied metrics describing the behavior of the remains of a stable double toroidal-helical vortex after its tearing off from the core of a stable vacuum formation.

The shortcomings of the mathematical model (i.e., the quasi-stable metrics used) do not allow us to calculate a number of important parameters of the phenomenon under study. For example, it is impossible to estimate the lifetime, velocity, and acceleration of the changing states of "neutrinos". It is not clear whether there is a limiting radius to which the radius of the throat of the scattering part of the "neutrino" can increase and a limiting radius to which the radius of the throat of the concentrating part of the "neutrino" can decrease, etc. An estimate of the

missing parameters of the mathematical model of the "neutrino" can only be obtained experimentally, possibly using the methods of generating the "neutrino" proposed in §§5 & 6.

At the same time, the mathematical model of "neutrino" used in this article does not contain restrictions on the scale of "neutrino". As already noted in §5, if in all the equations of this article instead of $r_6 \sim 10^{-13}$ cm (the radius of the cores of an elementary "particle", in particular the core of an "electron") we substitute any other radius r_j, then we will get "neutrino": molecular, cluster, cellular, planetary, galactic and other scales.

ACKNOWLEDGEMENTS

I sincerely thank Gavriel Davidov, David Reid, Tatyana Levy, Eliezer Rahman, David Kogan, Gennady Ivanovich Shipov, Evgeny Alekseevich Gubarev, Alexander Maslov, Alexander Bolotov, and Alexander Bindiman for their assistance. I thank David Johnson for providing an overview of the helical-toroidal electron concept.

REFERENCES

Abazajian, K.N., Acero, M.A., Agarwalla, S.K., Aguilar-Arévalo, A.A., Albright, C.H. Antusch, S, *et al*. (2012). Light sterile neutrinos. arXiv:1204.5379.

Adamson, F., Andreopoulus, C., Arms, K.E., Armstrong, R., Auty, D.J., Avvakumov, S., *et al*. (2007). Measuring the Speed of Neutrinos with the MINOS Detectors and the NuMI Neutrino Beam (Fermilab and University College London). *Phys. Rev. D 76* (7), 072005. doi: 10.1103/PhysRevD.76. 072005.

Alfonso, K., Artusa, D.R., Avignone, F.T., Azzolini, O., Balata, M., Banks, T.I, *et al*. (2015). Search for Neutrinoless Double-Beta Decay of ^{130}Te with CUORE-0. *Physical Review Letters*, *115* (10), 102502. arXiv:1504.02454.

Andrew, G., Cohen, A.G. & Glashow, S.L. (2011). New Constraints on Neutrino Velocities. *Phys. Rev. Lett., 107*, 181803, arXiv:1109.6562v1, https://doi.org/10.1103/PhysRevLett.107.181803.

Aničin, I. (2005). *The neutrino – its past, present, and future*. SFIN (Institute of Physics, Belgrade) Year XV. A: Conferences. 2: 3–59. arXiv:physics/0503172.

Abi, B., Acciarri, R., Acero, M.A., Adamov, G., Adams, D., Adinolfi, M., *et al*. (2020). Deep Underground Neutrino Experiment (DUNE), Far Detector Technical Design Report, Volume IV: Far Detector Single-phase Technology. *JINST, 15* (08), T08010, https://doi.org/10.1088/ 1748-0221/15/08/T08010.

Babu, K., Chauhan, G. & Dev, B. (2020). Neutrino nonstandard interactions via light scalars in the Earth, Sun, supernovae, and the early Universe. *Phys. Rev. D, 101* (9), 095029, https://doi.org/10.1103/PhysRevD. 101.095029.

Balantekin, A. (2011). Neutrino. *Physics Today, 64* (4), 58–60, https://doi.org/10.1063/1.3580495.

Batanov-Gaukhman, M. (2023a). Geometrized Vacuum Physics. Part I. Algebra of Stignatures. *Avances en Ciencias e Ingeniería, 14* (1), 1-26, https://www.executivebs.org/publishing.cl/avances-en-ciencias-e-ingenieria-vol-14-nro-1-ano-2023-articulo-1/; and Preprints, 2023060765. https://doi.org/10.20944/preprints202306.0765.v3, and viXra:2403.0035.

Batanov-Gaukhman, M. (2023b). Geometrized Vacuum Physics. Part II. Algebra of Signatures. *Avances en Ciencias e Ingeniería, 14* (1), 27-55, https://www.executivebs.org/publishing.cl/avances-en-ciencias-e-ingenieria-vol-14-nro-1-ano-2023-articulo-2/: and Preprints, 2023070716, https://doi.org/10.20944/preprints202307.0716.v1, and viXra:2403.0034.

Batanov-Gaukhman, M. (2023c). Geometrized Vacuum Physics. Part III. Curved Vacuum Area. *Avances en Ciencias e Ingeniería, 14* (2), 51-81, https://www.executivebs.org/publishing.cl/avances-en-ciencias-e-ingenieria-vol-14-nro-2-ano-2023-articulo-5/; and Preprints 2023, 2023080570. https://doi.org/10.20944/preprints202308. 0570.v4, and viXra:2403.0033.

Batanov-Gaukhman, M. (2023d). Geometrized Vacuum Physics. Part IV: Dynamics of Vacuum Layers. *Avances en Ciencias e Ingeniería, 14* (3), 1-29, 31-87, https://www.executivebs.org/publishing.cl/avances-en-ciencias-e-ingenieria-vol-14-nro-3-ano-2023-articulo-1/, and Preprints.org. https://doi.org/10.20944/preprints202310.1244.v3, and viXra:2403.0032.

Batanov-Gaukhman, M. (2023e). Geometrized Vacuum Physics Part V: Stable Vacuum Formations, *Avances en Ciencias e Ingeniería, 14* (3), 31-87, https://www.executivebs.org/publishing.cl/avances-en-ciencias-e-ingenieria-vol-14-nro-3-ano-2023-articulo-2/ and viXra:2405.0002 .

Batanov-Gaukhman, M. (2023f). Geometrized Vacuum Physics Part VI: Hierarchical Cosmological Model, *Avances en Ciencias e Ingeniería, 14* (4), 27-76, https://www.executivebs.org/publishing.cl/avances-en-ciencias-e-ingenieria-vol-14-nro-4-ano-2023-articulo-3/ and viXra:2408.0010.

Batanov-Gaukhman, M. (2024a). Geometrized Vacuum Physics Part VII: "Electron" and "Positron", *Avances en Cien-cias e Ingeniería, 15* (1), 23-69, https://www.executivebs.org/publishing.cl/avances-en-ciencias-e-ingenieria-vol-15-nro-1-ano-2024-articulo-3/ and viXra:2409.0097.

Batanov-Gaukhman, M. (2024b) Geometrized Vacuum Physics. Part VIII: Inertial Electromagnetism of Moving «Particles», *Avances en Ciencias e Ingeniería, 15* (2), 1-36, https://www.executivebs.org/publishing.cl/avances-en-ciencias-e-ingenieria-vol-15-nro-2-ano-2024-articulo-1/ and viXra:2411.0086.

Batanov, M. (2006). *Volkov effect* // Proceedings of the conference "Synergetics vol. 8" - M: Moscow State University.

Bellerive, A., Klein, J.R., McDonald, A.B., Noble, A.J. & Poon, A.W.P. (2016). The Sudbury Neutrino Observatory. *Nuclear Physics B*, *908*, 30–51. arXiv:1602.02469. doi:10.1016/j.nuclphysb.2016.04.035.

Bobrov, A.V. (2007). *Model studies of the field concept of the mechanism of consciousness*. - Orel: Orel State Technical University.

Close, F. (2010). *Neutrino*. Published in the United States by Oxford University Press Inc., New York ISBN 978-0-19-957459-9.

Cooper, K. (2022). *What are neutrinos*? Space.com.

Criado, J. & Feruglio, F. (2018). Modular Invariance Faces Precision Neutrino Data. *SciPost Phys., 5* (5), 042. arXiv:1807.01125.

Ding, G-J., Lui, Liu, X-G. & Yao, C-Y. (2022). A minimal modular invariant neutrino model, arXiv:2211.04546, DOI: 10.48550/arXiv.2211.04546.

Feruglio, F. & Romanino, A. (2021). Lepton flavor symmetries. *Rev. Mod. Phys., 93* (1), 015007. arXiv:1912.06028.

Gu, P-H., Ma, E. & Sarkar, U. (2016). Connecting Radiative Neutrino Mass, Neutron-Antineutron Oscillation, Proton Decay, and Leptogenesis through Dark Matter. *Phys. Rev. D, 94* (11), 111701.

Johnson, C. & Tegen, R. (1999). The little neutral one: An overview of the neutrino. *South African Journal of Science*, 95 (95), 13–20. hdl:10520/AJA00382353_7822.

King, S. (2017). Unified Models of Neutrinos, Flavour and CP Violation. *Prog. Part.Nucl. Phys. 94217*–256, arXiv:1701.04413.

Kobayashi, T., Tanaka, K. & Tatsuishi, T. (2018). Neutrino mixing from finite modulargroups. *Phys. Rev. D, 98* (1), 016004. arXiv:1803.10391.

Kolbe, E., Langanke, K. & Fuller, G. (2004). Neutrino-Induced Fission of Neutron-Rich Nuclei. *Physical Review Letters,* 92 (11), 111101. arXiv:astro-ph/0308350.

Kostelecký, V. & Mewes, M. (2004). Lorentz and CPT violation in neutrinos. *Phys. Rev. D, 69* (1), 016005. arXiv:hep-ph/0309025.

Lasserre, T. (2014). Light sterile neutrinos in particle physics: Experimental status. *Physics of the Dark Universe, 4*, 81–85. arXiv:1404.7352. doi:10.1016/j.dark.2014.10.001.

Lesgourgues, J. & Pastor, S. (2006). Massive neutrinos and cosmology. *Phys. Rept., 429*, 307, 307-379. arXiv:astro-ph/0603494.

Marinov, K., Boardman, A. & Fedotov, V. (2007). Metamaterial Toroidal. *New Journal of Physics, 9*, 324–335.

Medvedeva, A.A. & Panchelyuga, V.A. (2014). Volkov effect // Metaphysics, 2014, No. 1 (11).

Mertens, S. (2016). *Direct Neutrino Mass Experiments*. arXiv:1605.01579. S2CID 56355240. NuPhys2015, Prospects in Physics Barbican Centre, London, UK, December 16–18, 2015.

Nomura, T. & Popov, O. (2024). Extended Scotogenic Model of Neutrino Mass and Proton Decay. arXiv:2406.00651v1.

Shao, Y., Du, G.H., Li, T.N. & Zhang, X. (2025). Prospects for measuring neutrino mass with 21-cm forest. arXiv:2501.00769.

Shipov, G. (1998). *A Theory of Physical Vacuum*. Moscow ST-Center, Russia ISBN 5 7273-0011-8.

Suematsu, D. (2024). *Neutrino models with a zero mass eigenvalue*. arXiv:2412.05774.

Winter, K. (2000). *Neutrino Physics*. Cambridge University Press. ISBN 978-0-521-65003-8.

Wolfenstein, L. (1978). Neutrino Oscillations in Matter. *Phys. Rev. D, 17*, 2369–2374. https://doi.org/10.1103/PhysRevD.17.2369.

Worcester, E. (2023). The Dawn of Collider Neutrino Physics. *Physics, 16*, 113. doi:10.1103/Physics.16.113.S2CID 260749625.

Valentino, E., Gariazzo, S., Giar`e, W. & Mena, O. (2023). Impact of the damping tail on neutrino mass constraints. *Phys. Rev. D, 108*, 083509, arXiv:2305.12989.